In-Situ Stress and Fractures

En-Chao Yeh[1], Wei-Cheng Li[1], Felix Fang-Yih Wu[1], Chao-Yan Lin[1], Ping-Chuan Chen[1], Chi-Shun Shui[1], Tsu-En Kao[1], Tien-Hsiang Sun[1], Shih-Ting Lin[2], Weiren Lin[3], Tai-Tien Wang[4], Jih-Hao Hung[5], Yoshitaka Hashimoto[6], Yih-Min Wu[2], Sheng-Rong Song[2], Chien-Ying Wang[5], Wayne Lin[7],Chi-Wen Yu[8], Chung-Hui Chiao[9], Ming-Wei Yang[10], Chen-Kuo Lin[7]

1 Department of Earth Sciences, National Taiwan Normal University, Taipei, Taiwan
2 Department of Geosciences, National Taiwan University, Taipei, Taiwan
3 Graduate School of Engineering, Kyoto University, Japan
4 Institute of Mineral Resources Engineering, National Taipei University of Technology, Taipei, Taiwan
5 Institute of Geophysics, National Central University, Taiwan
6 Department of Applied Science, Faculty of Science, Kochi University, Kochi, Japan
7 Green Energy and Environment Research Laboratories, Industrial Technology Research Institute, Hsinchu, Taiwan
8 Sinotech Engineering Consultants Inc., Taipei, Taiwan
9 Taiwan Power Company, Taipei, Taiwan
10 Taiwan Power Research Institute, Taipei, Taiwan

Take-Home Messages

- Integrated stress assessments from various methods, it will be able to determine the stress state in multiple spatial scales and stress gradient.
- Mechanical relationship between in-situ stress and fracture should be able to apply for various topics of solid earth sciences.

Outline

- Importance of Stress State for fracture
- Stress Determination
- Case Study
  - CCS
  - TCDP
  - Waste Disposal
  - Geothermal Wells
- Summary

Importance of Stress State

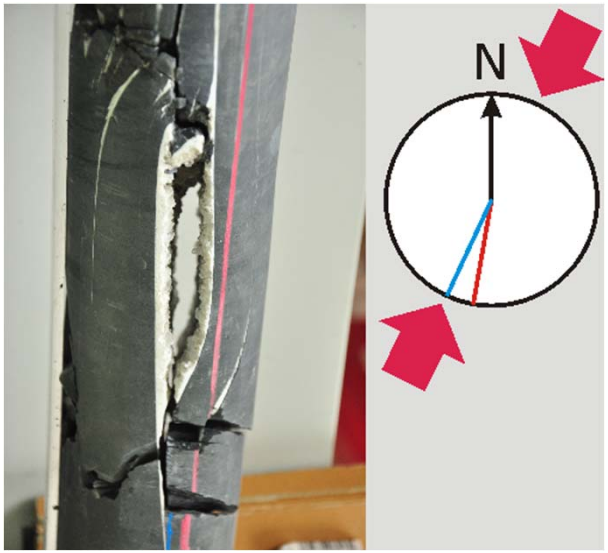

Enhanced Geothermal System

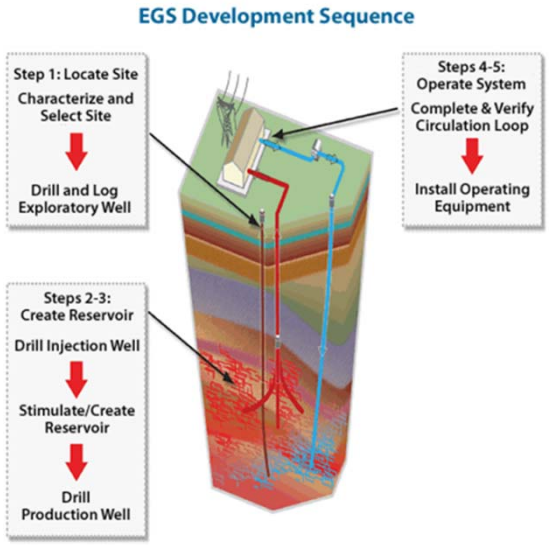

Petroleum Drilling

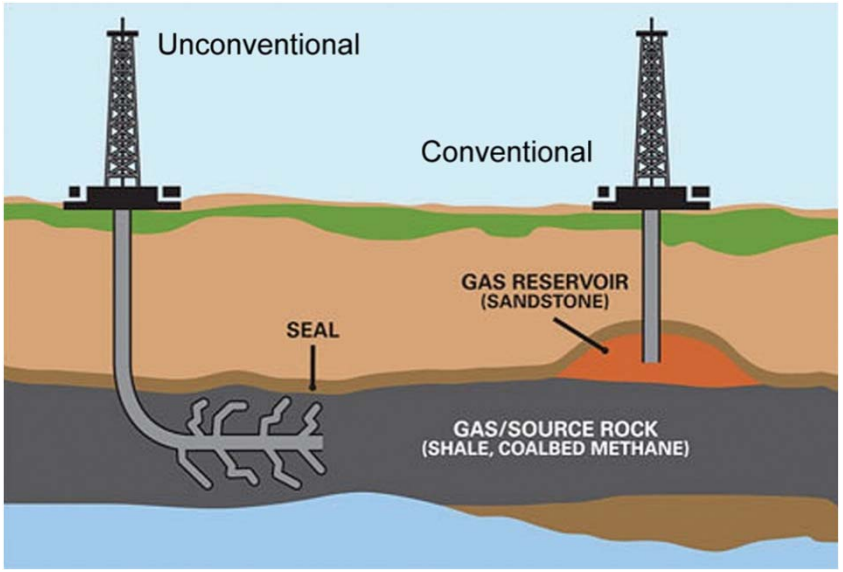

Waste Disposal

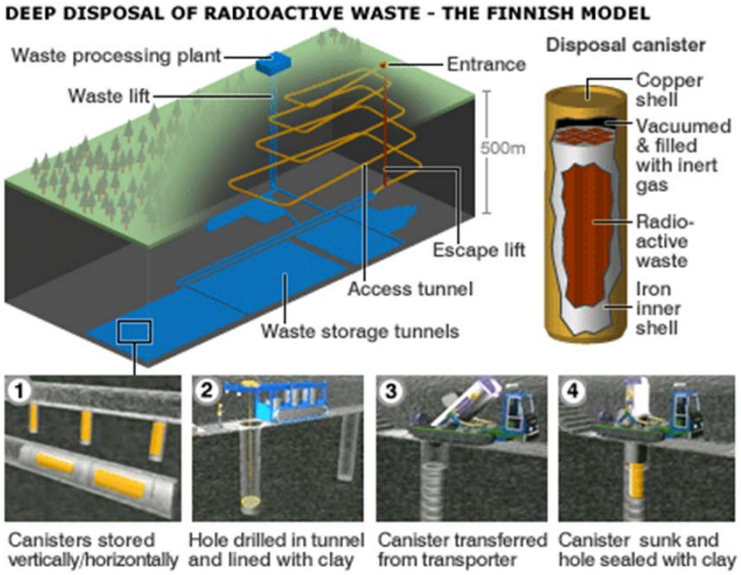

Carbon Dioxide Sequestration

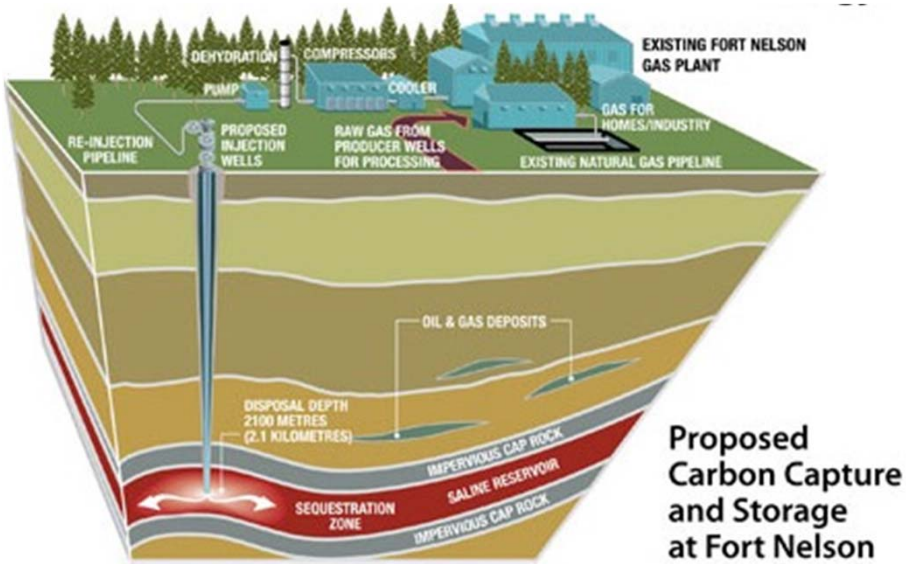

Proposed Carbon Capture and Storage at Fort Nelson

Geoengineering

Subduction Zone

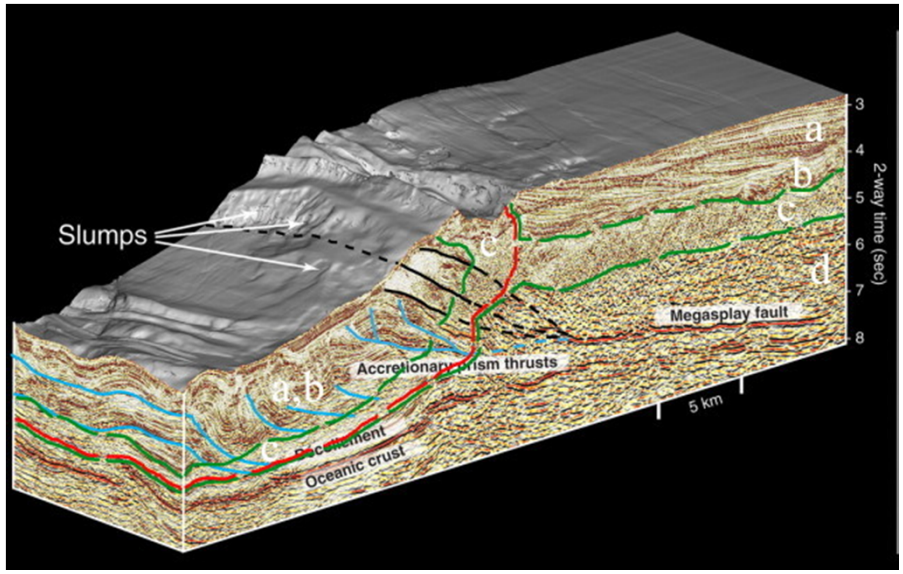

Fault Reactivation

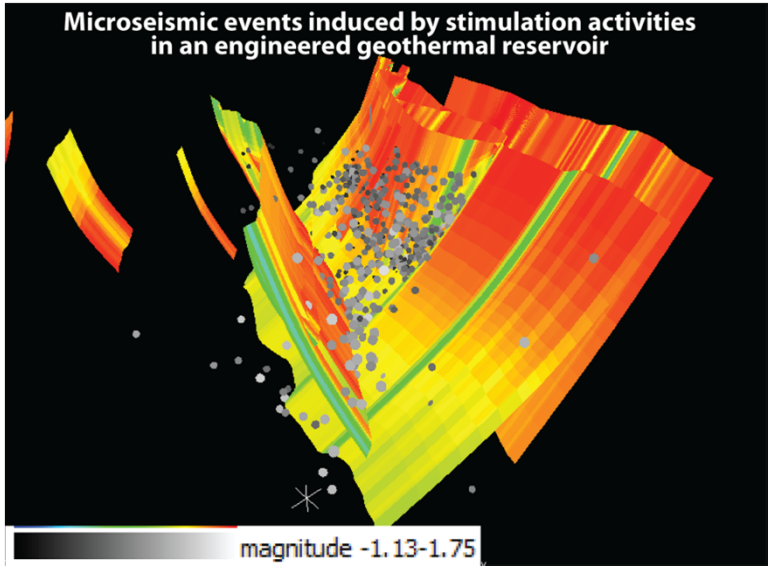

Mantle Flow

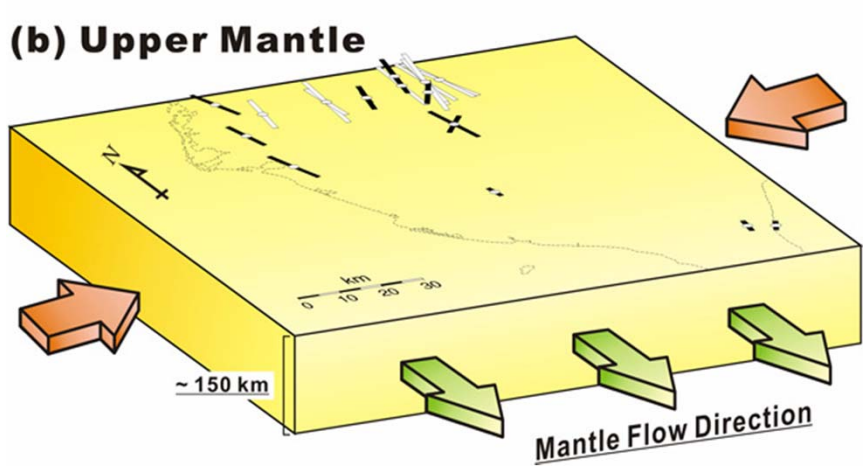

Strain & Stress Determination

- GPS velocity field (GPS)
- Focal mechanism (FM)
- Fault slip inversion (FS)
- Bore-based methods
  - Breakout (BO), Drilling-Induced Tensile Fracture (DIFT), Hydraulic Fracturing (HF),…..
- Core-based methods
  - Anelastic Strain Recovery (ASR), Acoustic Emission (AE), Deformation Core Diameter Analysis (DCDA), Core Observation (CO),….

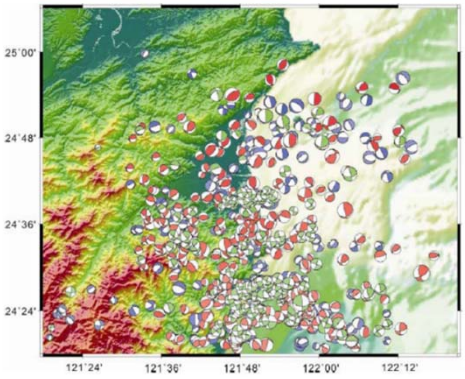

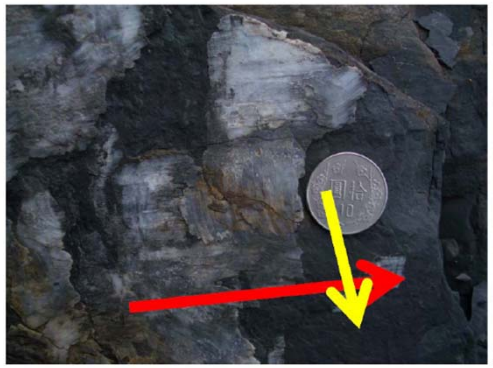

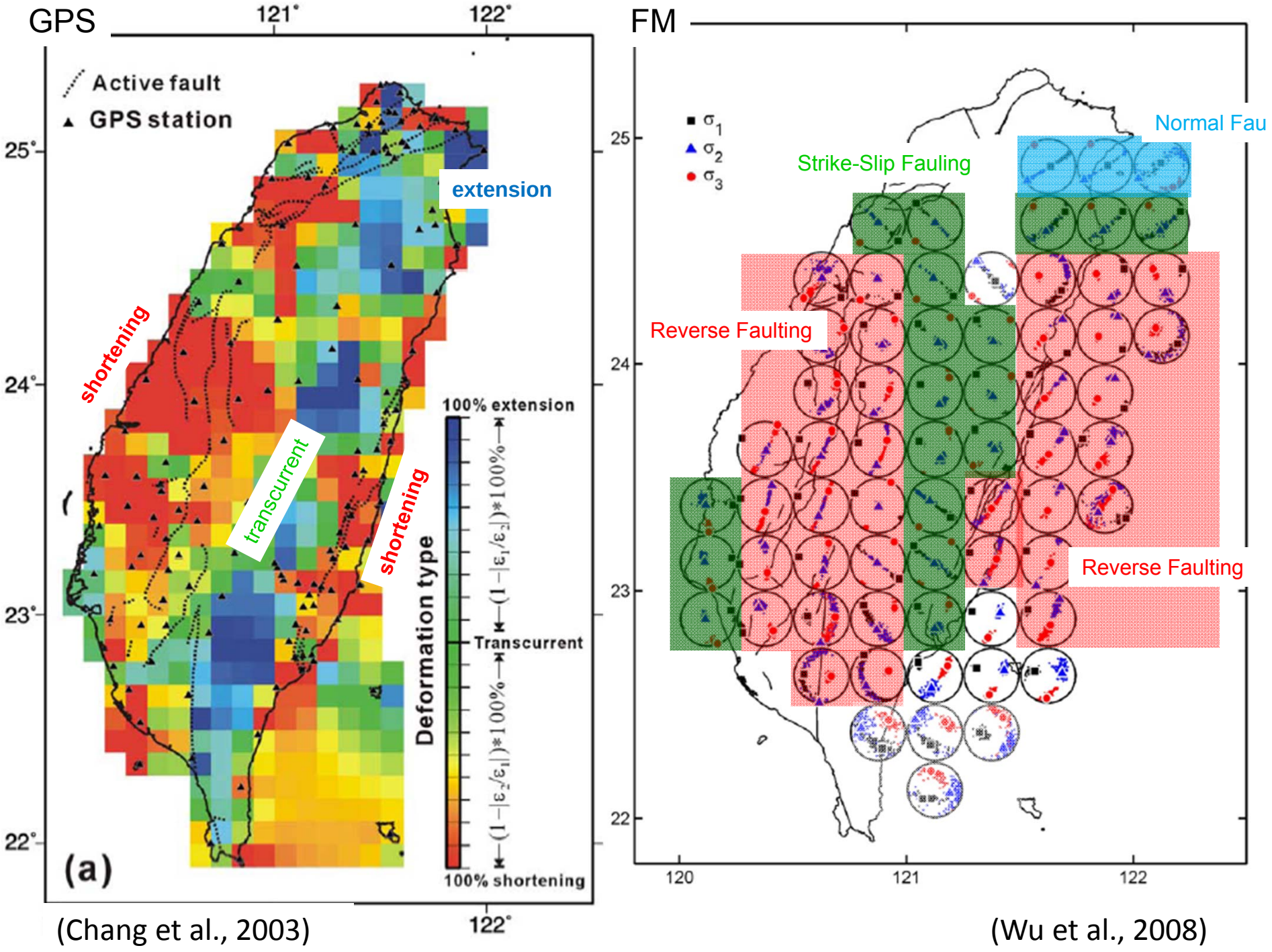

(Chang et al., 2003)

(Wu et al., 2008)

Geomechanical model
Stress observation from borehole failure

Borehole Structures & Stress
(Vertical Borehole)

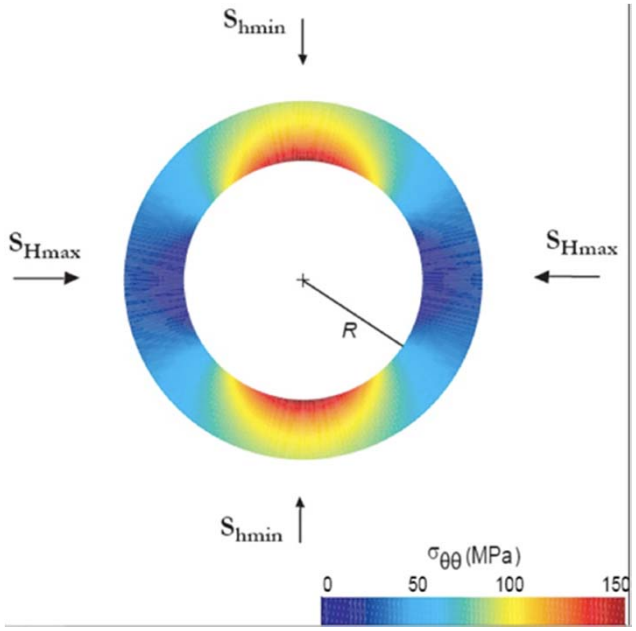

Stress Concentration
At Borehole Wall

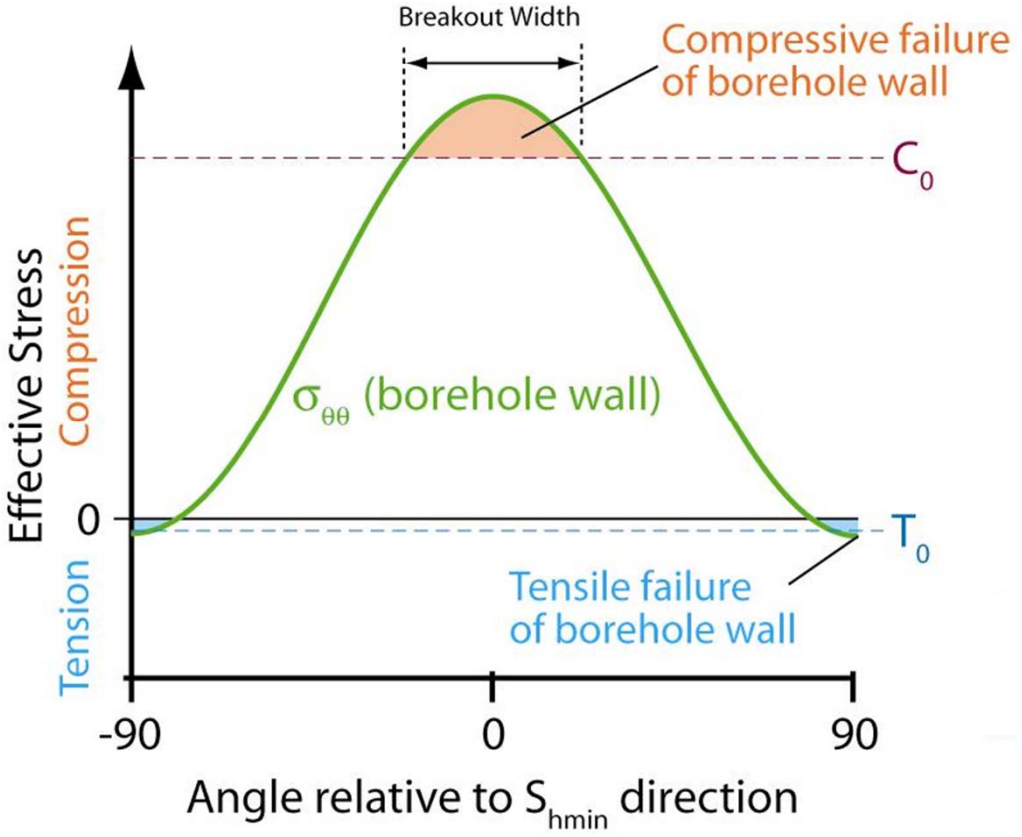

From N.C. Davatzes

Borehole Image

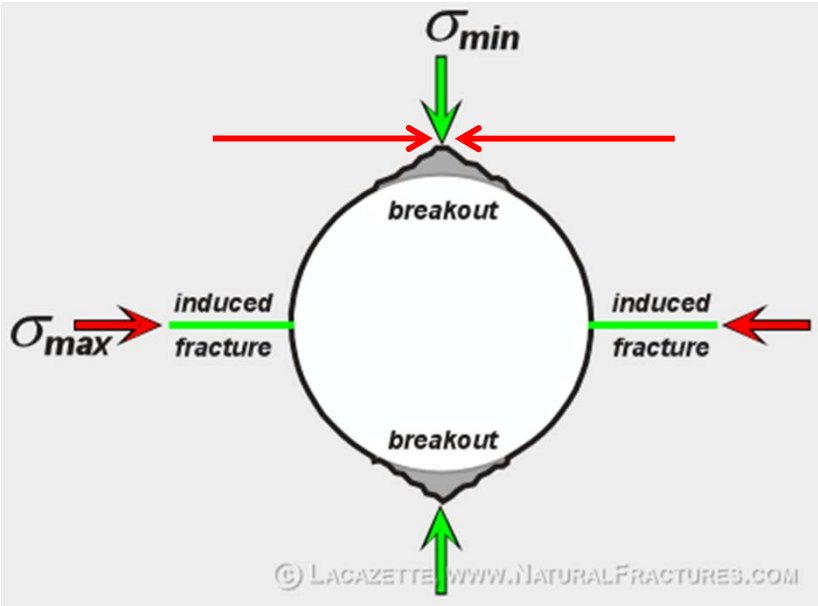

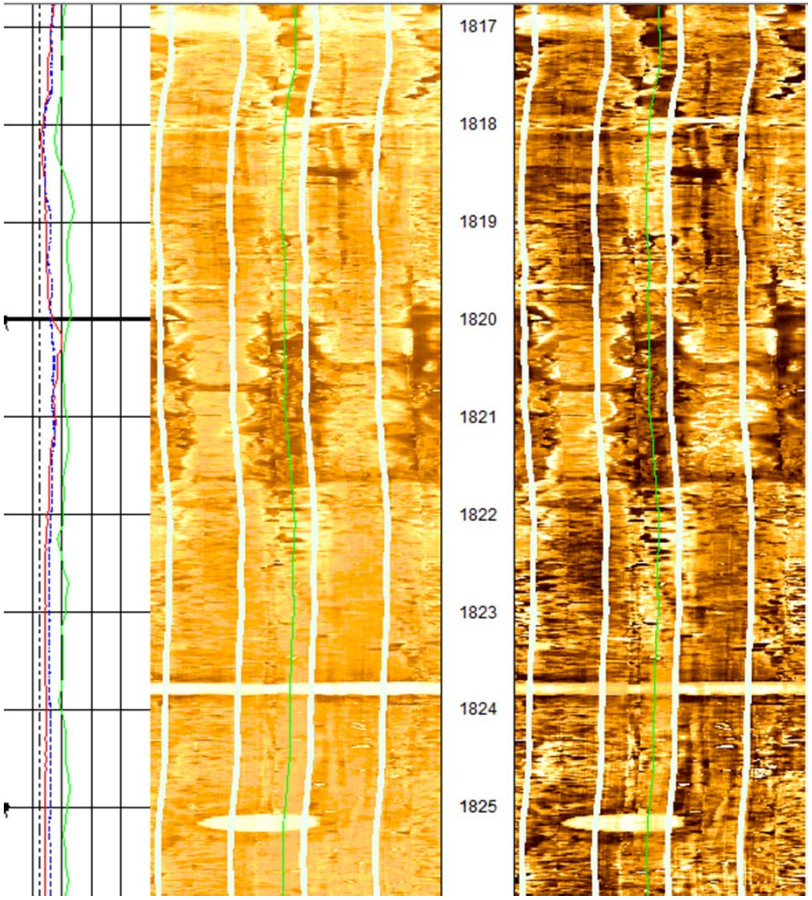

DIFT

BO

Stress Polygon

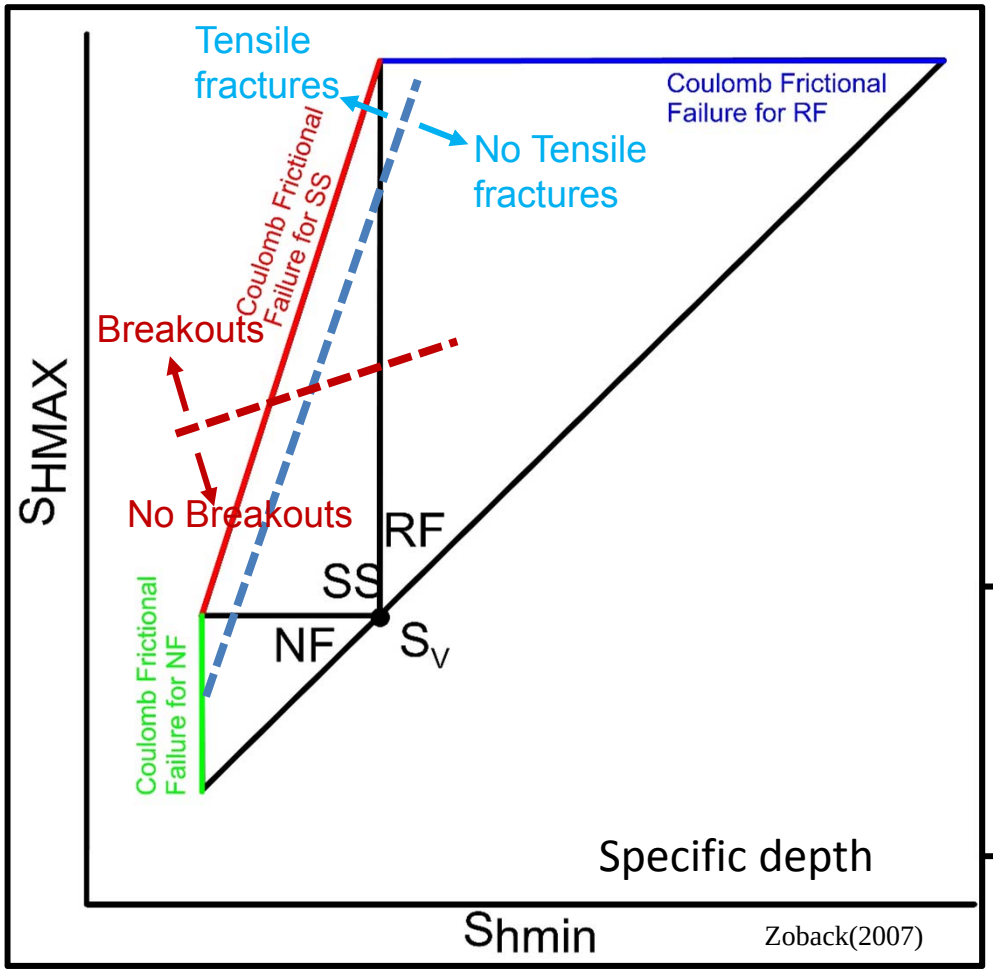

Normal Faulting

$$\frac{\sigma_1}{\sigma_3} = \frac{S_V - PP}{S_{hmin} - PP} \leq \left(\sqrt{1+\mu^2} + \mu\right)^2$$

Reverse Faulting

$$\frac{\sigma_1}{\sigma_3} = \frac{S_{Hmin} - PP}{S_V - PP} \leq \left(\sqrt{1+\mu^2} + \mu\right)^2$$

Strike-Slip Faulting

$$\frac{\sigma_1}{\sigma_3} = \frac{S_{Hmax} - PP}{S_{hmin} - PP} \leq \left(\sqrt{1+\mu^2} + \mu\right)^2$$

$$T_0 = 3S_{hmin} - S_{Hmax} - 2P_p - \Delta P$$

$$C_0 = (1 - 2cos2\theta_b)S_{Hmax} + (1 + 2cos2\theta_b)S_{hmin} - 2P_p$$

$$2\theta_b = \pi - w_{b_0}$$

C_0: uniaxial compressive strength

Hydraulic Fracturing (HF)

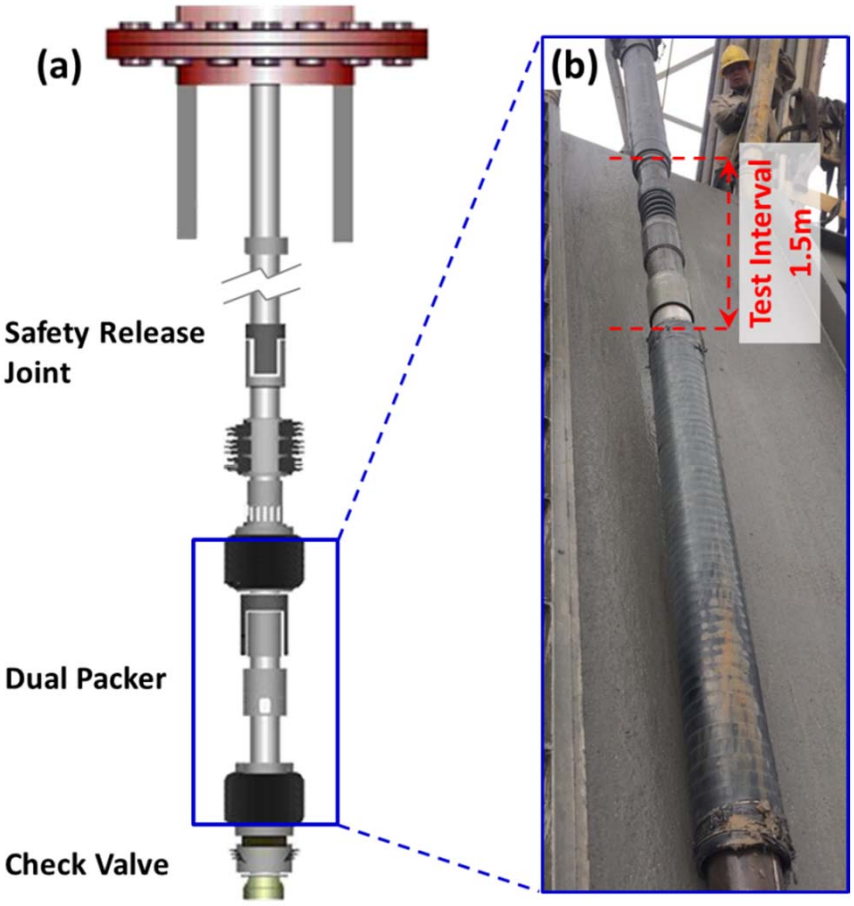

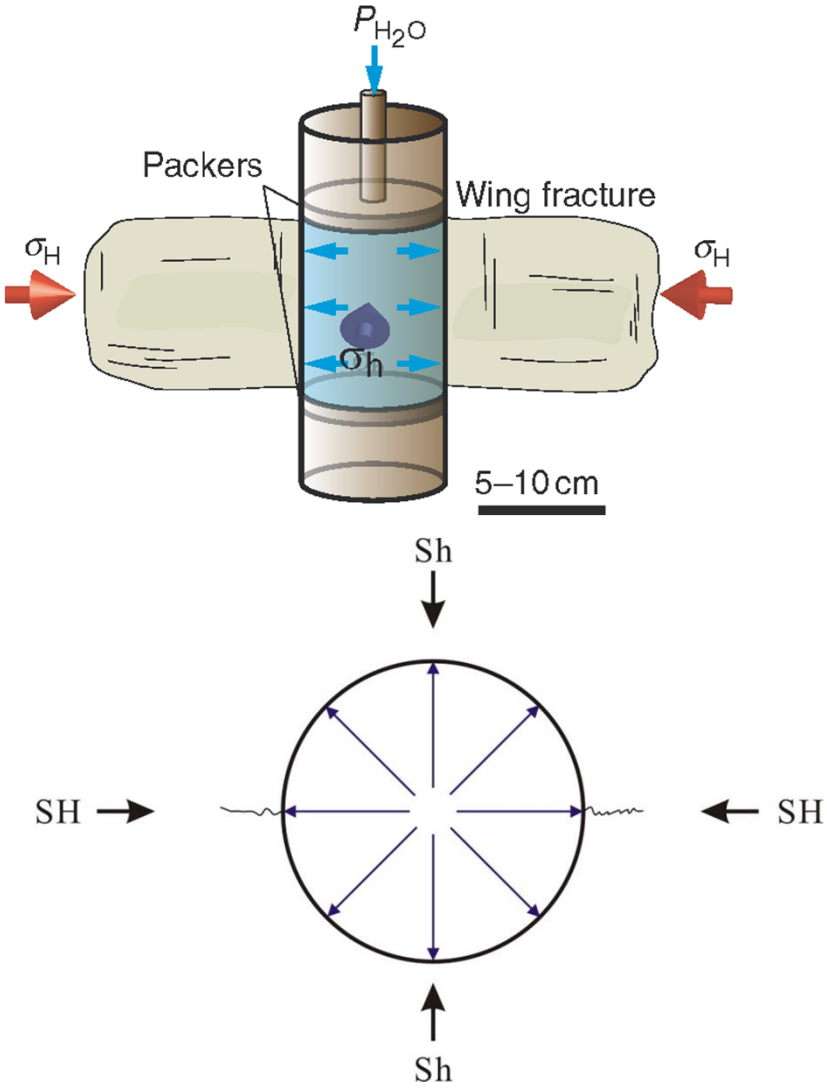

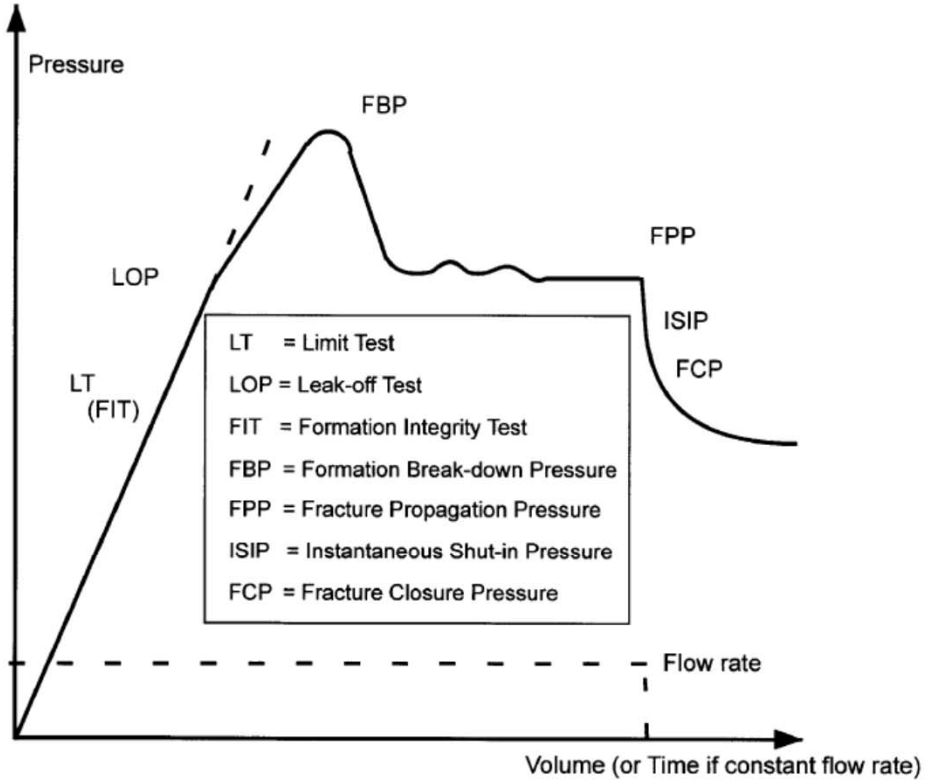

Fig. 4. Schematic illustration of an extended LOT (after Gaarenstroom et al. [22]). The various terms associated with such a test are explained in the text.

Zoback *et al.*,(2003)

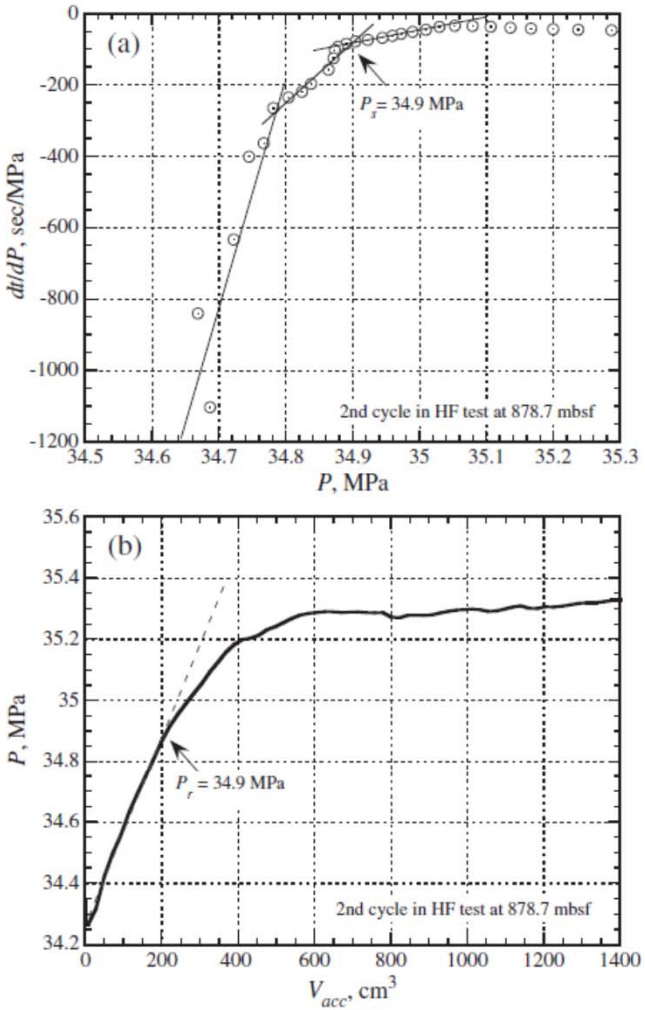

Figure 5. (a) Plot of dt/dP versus P obtained from the pressure decay curve after shut-in and (b) P-V_{acc} curve at the second pressurization cycle in the HF test at 878.7 mbsf.

Ito *et al.*,(2013)

Stress Release

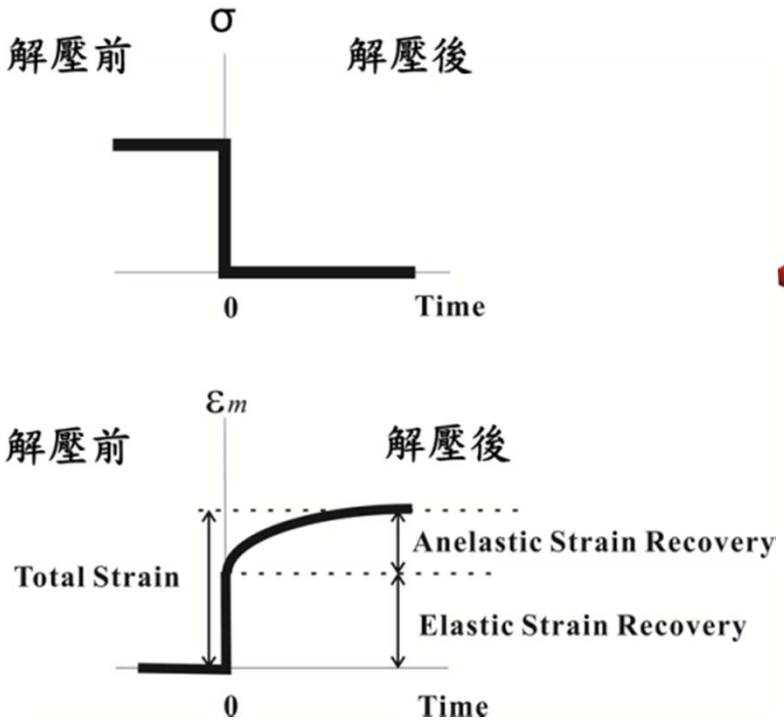

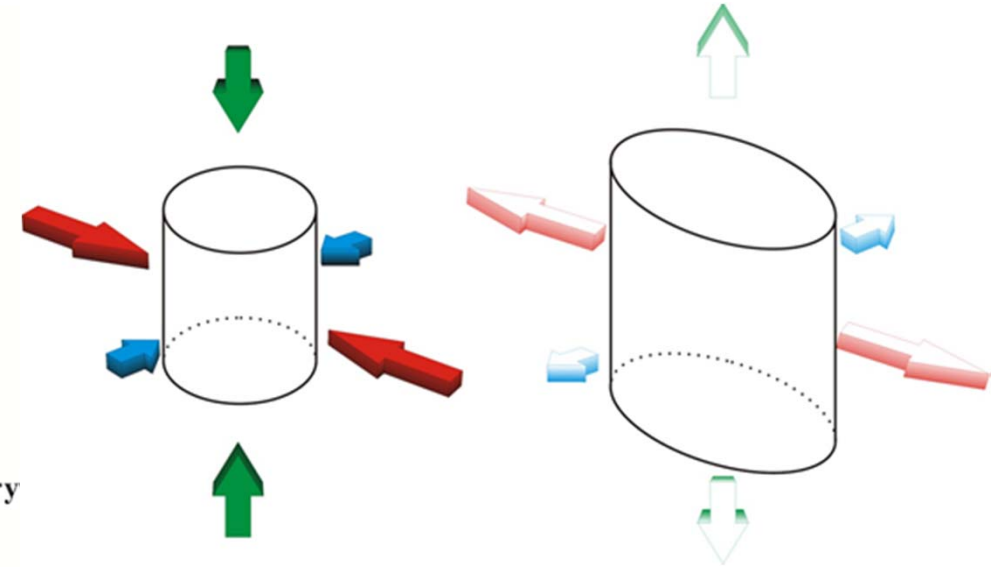

Anelastic Strain Recovery (ASR)

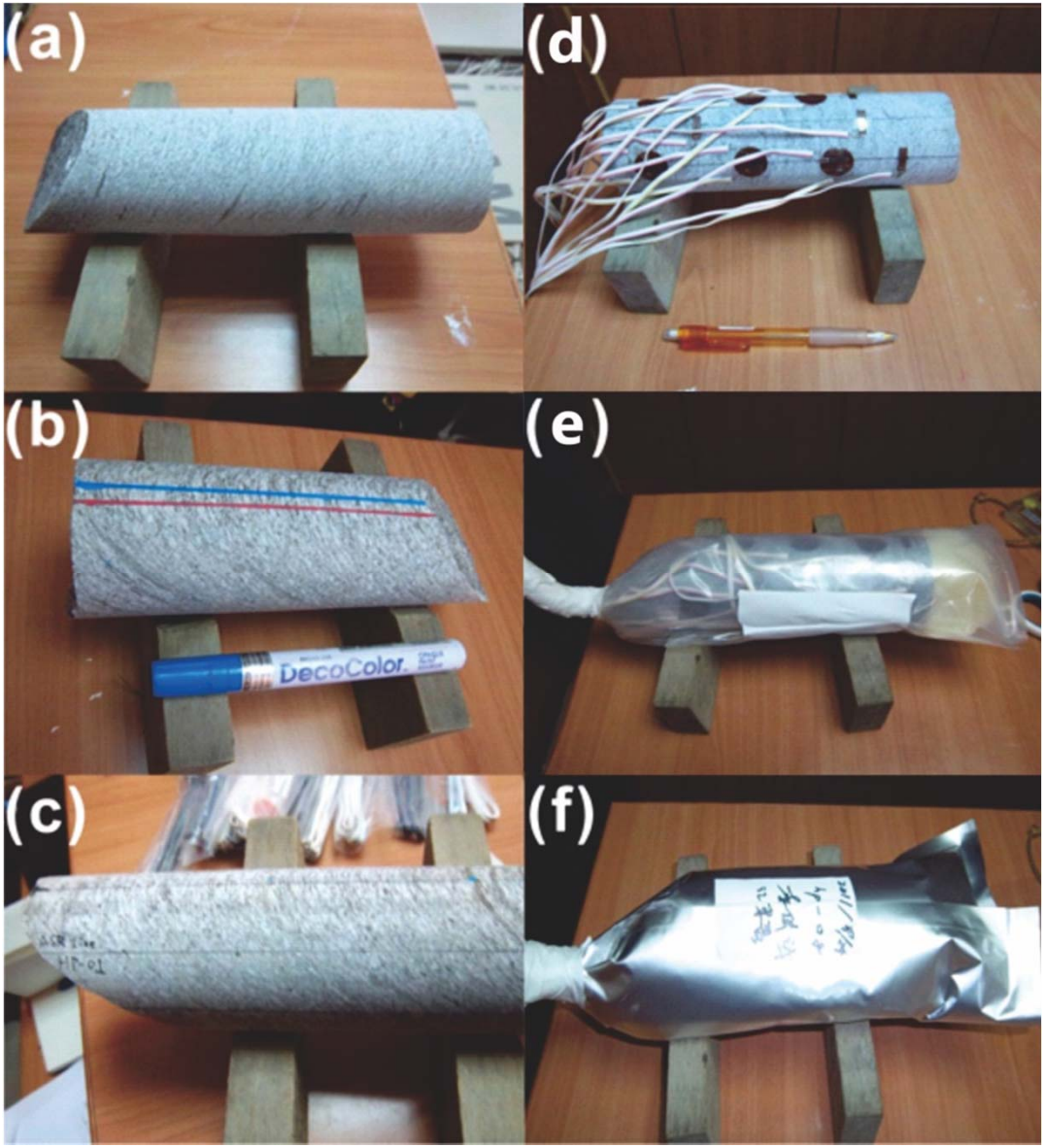

$$(\varepsilon) = \begin{bmatrix} \varepsilon_{xx} & \varepsilon_{xy} & \varepsilon_{xz} \\ \varepsilon_{yx} & \varepsilon_{yy} & \varepsilon_{yz} \\ \varepsilon_{zx} & \varepsilon_{zy} & \varepsilon_{zz} \end{bmatrix} \begin{Bmatrix} l \\ m \\ n \end{Bmatrix}$$

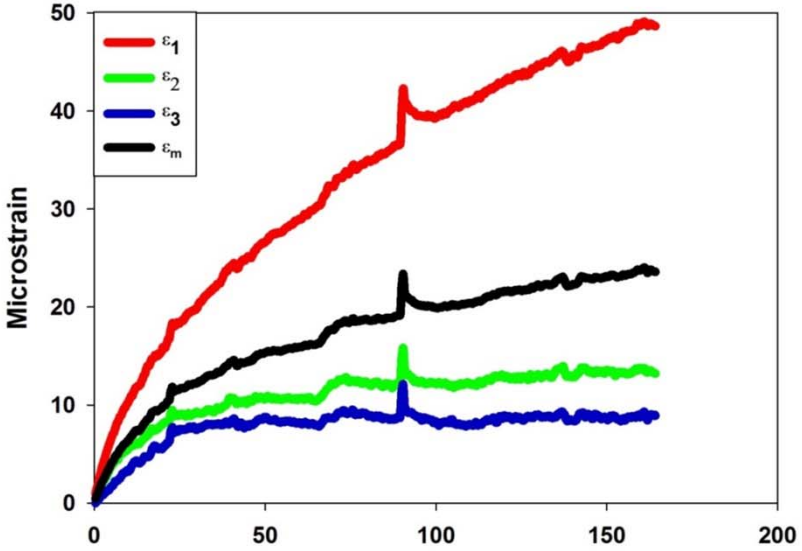

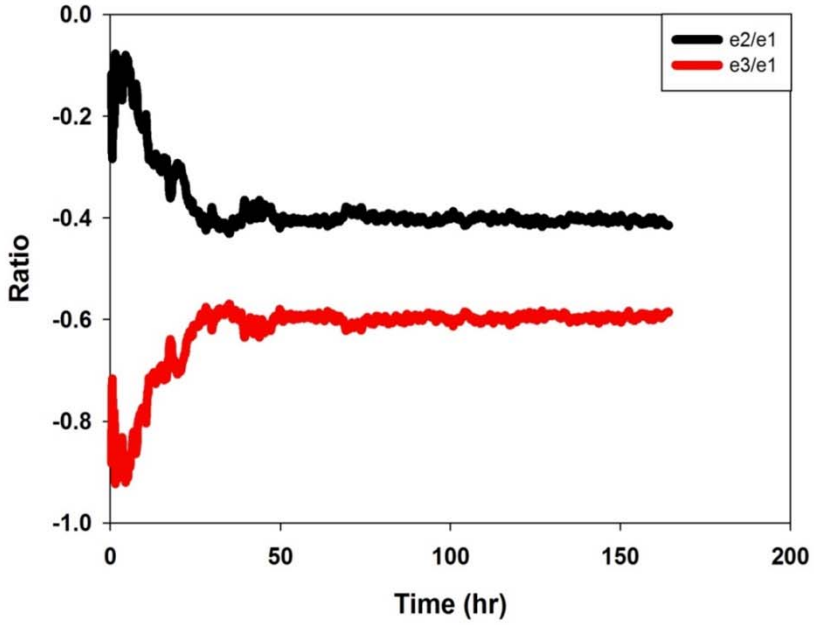

$$(\varepsilon) = \begin{bmatrix} \varepsilon_{xx} & \varepsilon_{xy} & \varepsilon_{xz} \\ \varepsilon_{yx} & \varepsilon_{yy} & \varepsilon_{yz} \\ \varepsilon_{zx} & \varepsilon_{zy} & \varepsilon_{zz} \end{bmatrix} \begin{Bmatrix} l \\ m \\ n \end{Bmatrix} = \begin{bmatrix} \varepsilon_n & 0 & 0 \\ 0 & \varepsilon_n & 0 \\ 0 & 0 & \varepsilon_n \end{bmatrix} \begin{Bmatrix} l \\ m \\ n \end{Bmatrix}$$

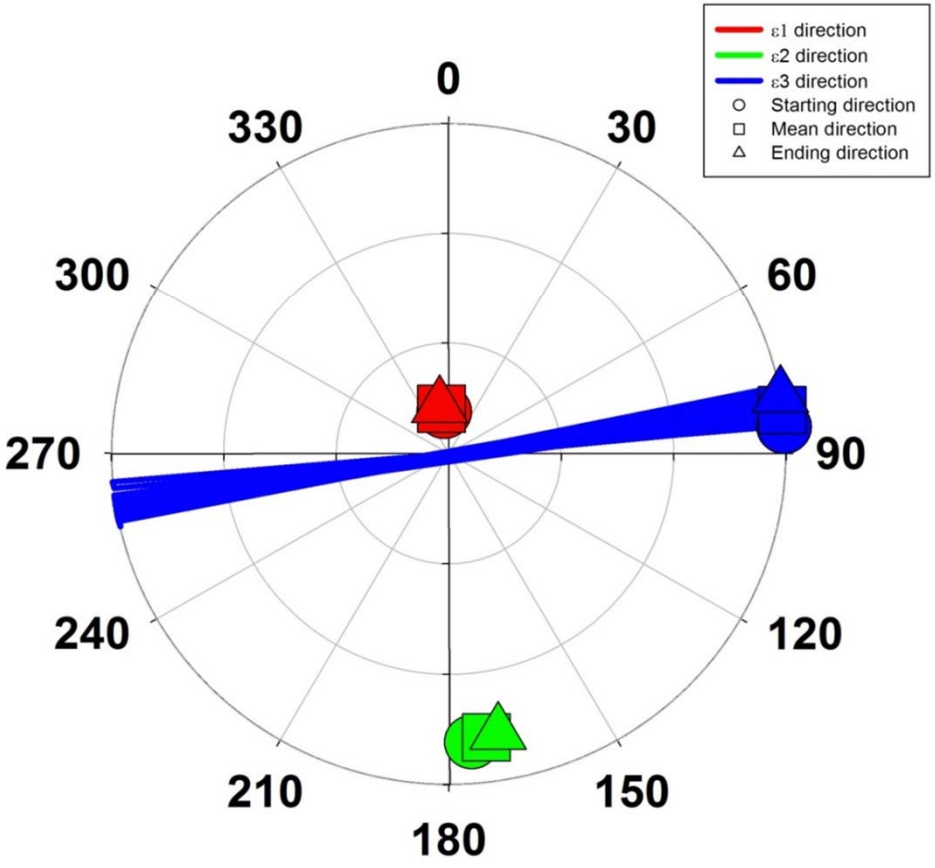

$$\sigma_{ij} = C_{ijkl}\, \varepsilon_{kl}$$

Deformation Core Diameter Deformation (DCDA)

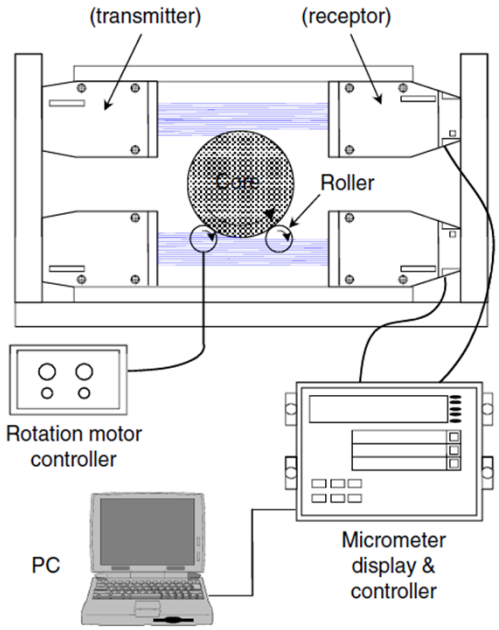

(Takatoshi et al.,2013)

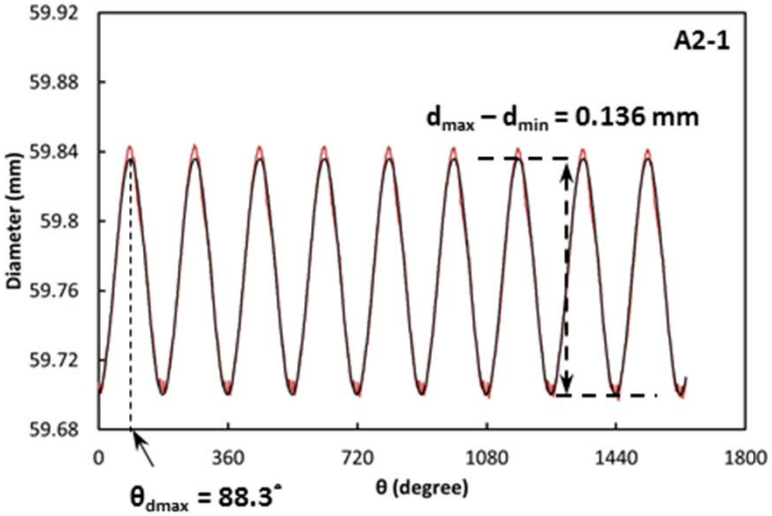

$$d_\theta = \frac{d_{max}+d_{min}}{2} + \frac{d_{max}-d_{min}}{2} * \cos(\theta - \alpha)$$

$$S_{Hmax} - S_{hmin} = \frac{(d_{max} - d_{min})}{d_0} * \frac{E}{1+\nu}$$

Acoustic Emission

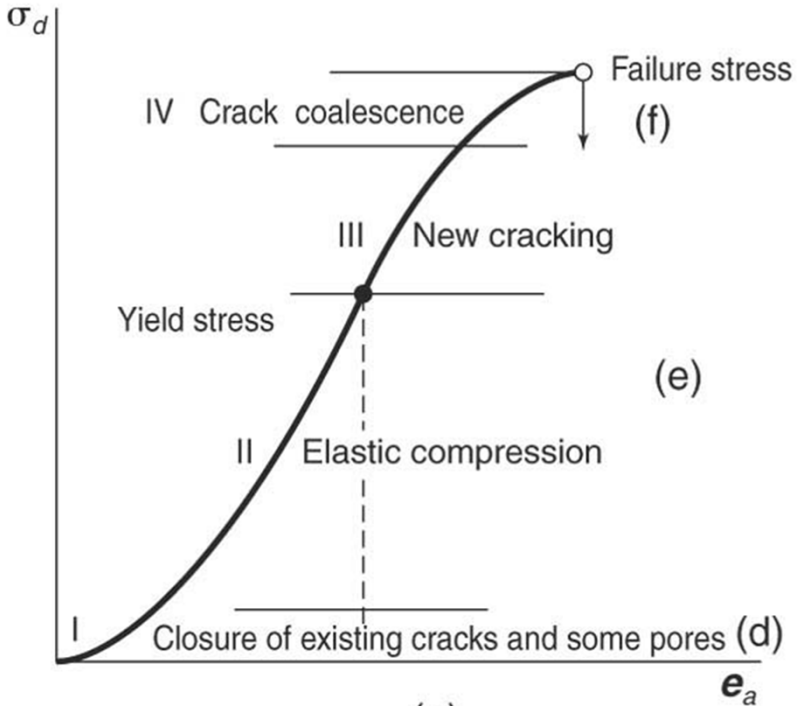

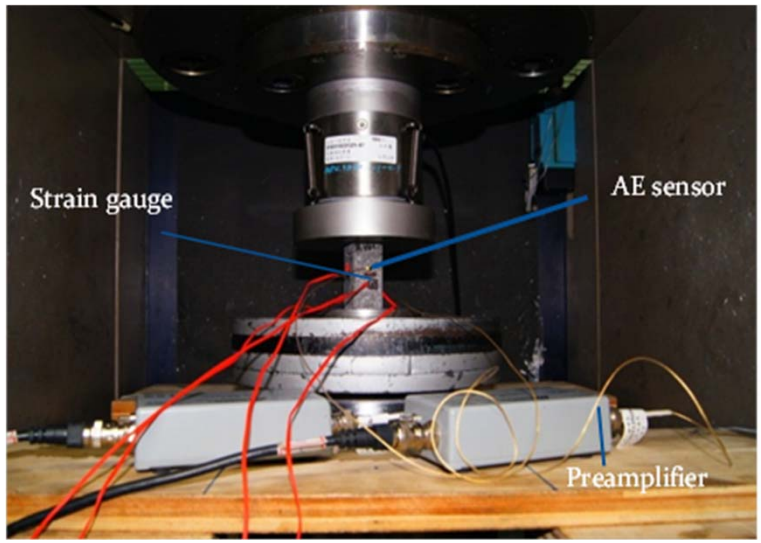

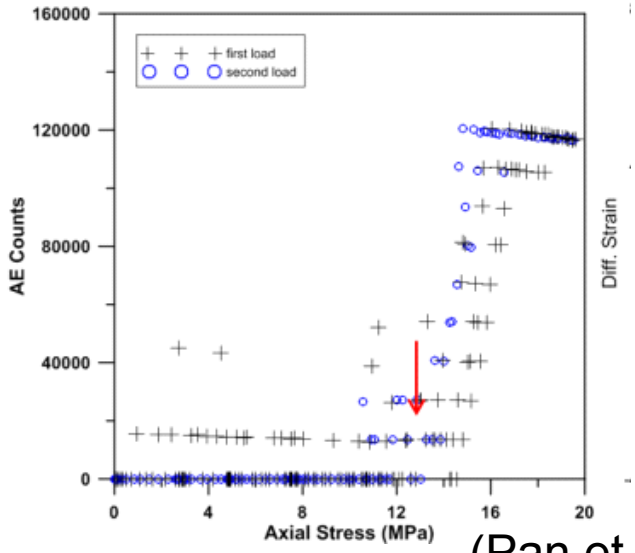

(Pan et al., 2013)

Principal Stress

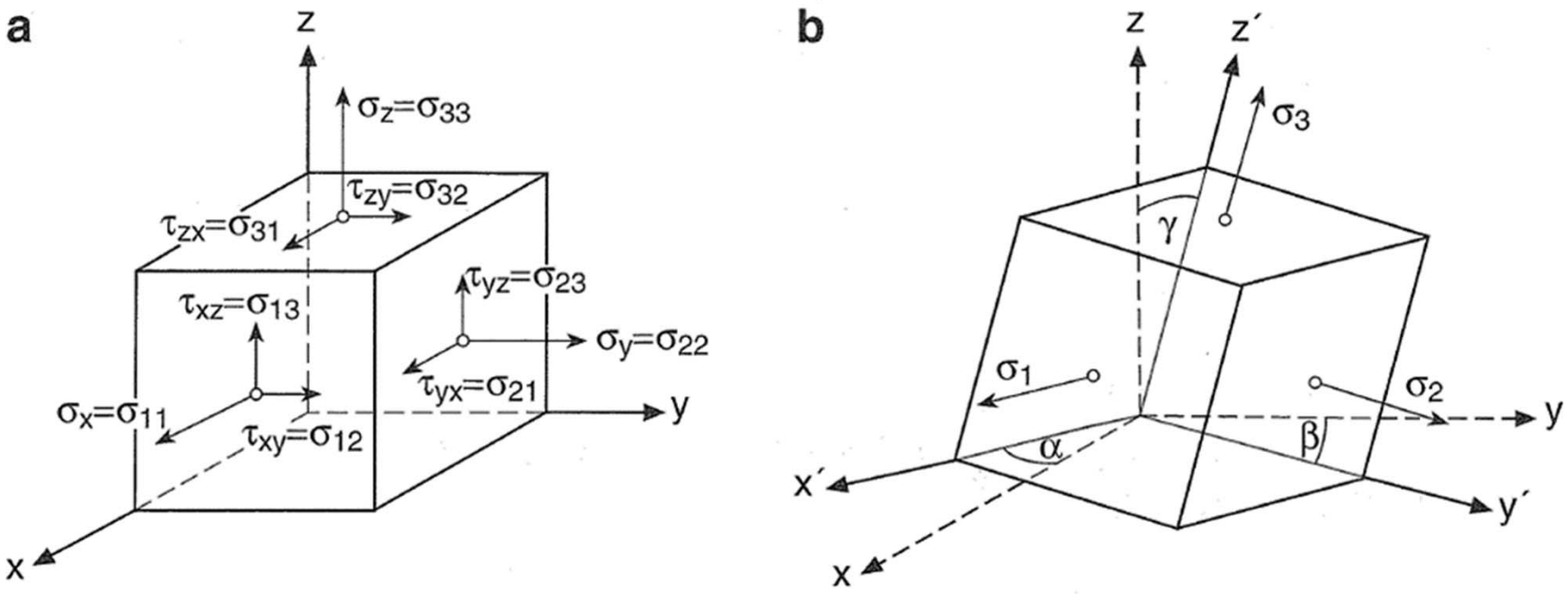

Fig. 2.4 Visualization of stress components in 3D on a cube **a** before and **b** after solving the eigenvalue problem of the stress matrix; engineering mechanics notation (tension positive convention)

Anderson's theory of faulting

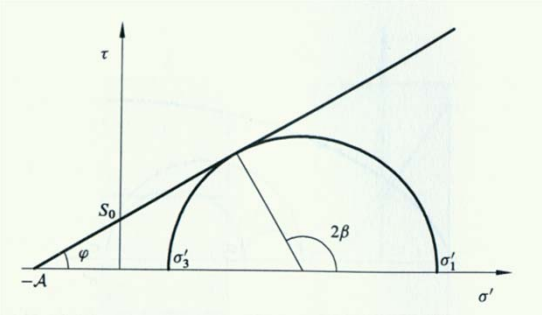

- $2\theta + \phi = 90^0$
- $\phi \sim 30^0$

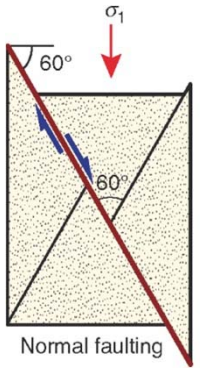

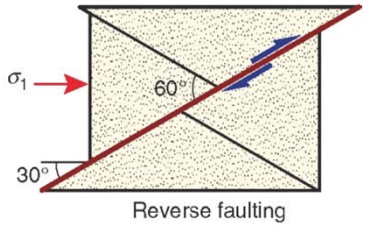

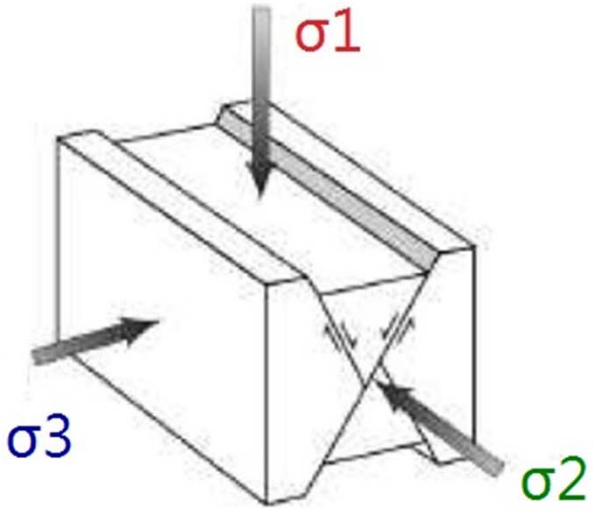

Normal Faulting
NF

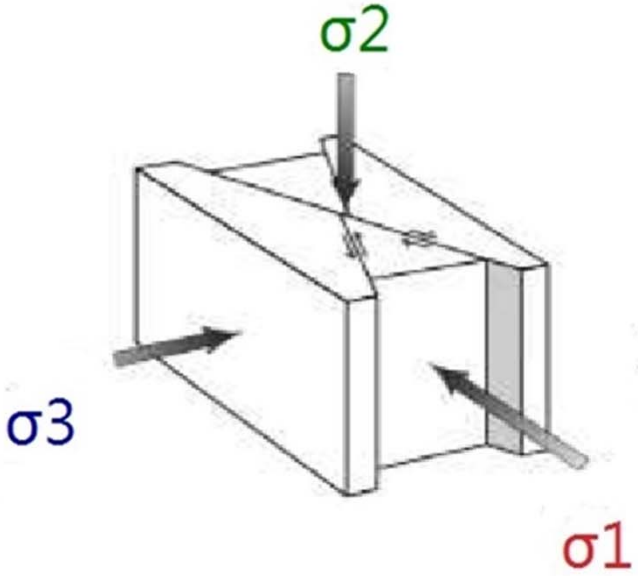

Strike-Slip Faulting
SS

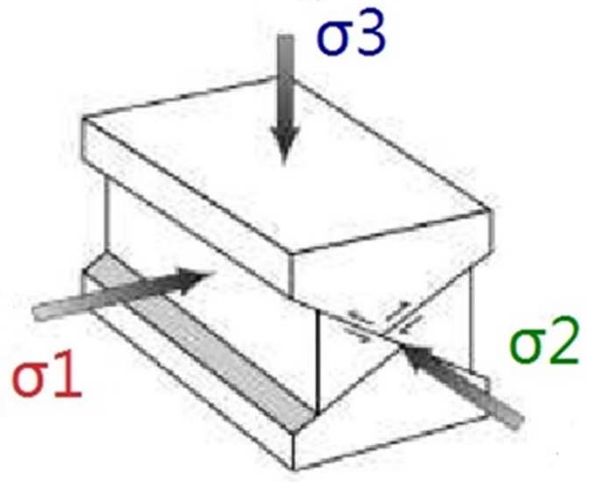

Reverse Faulting
RF

(Anderson 1951)

Slip & Dilation Tendency

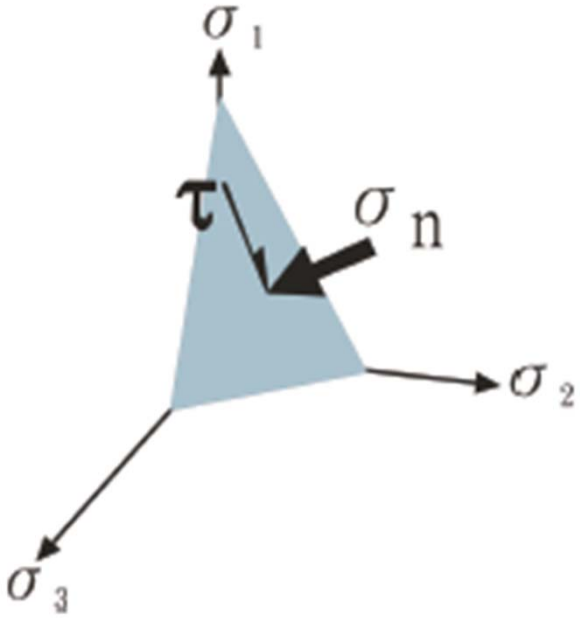

$$Ts = \frac{\tau}{\sigma_n'} \geq \mu$$

$$T_d = \frac{\sigma_1 - \sigma_n}{\sigma_1 - \sigma_3}$$

(Morris et al., 1996; Ferrill et al., 1999)

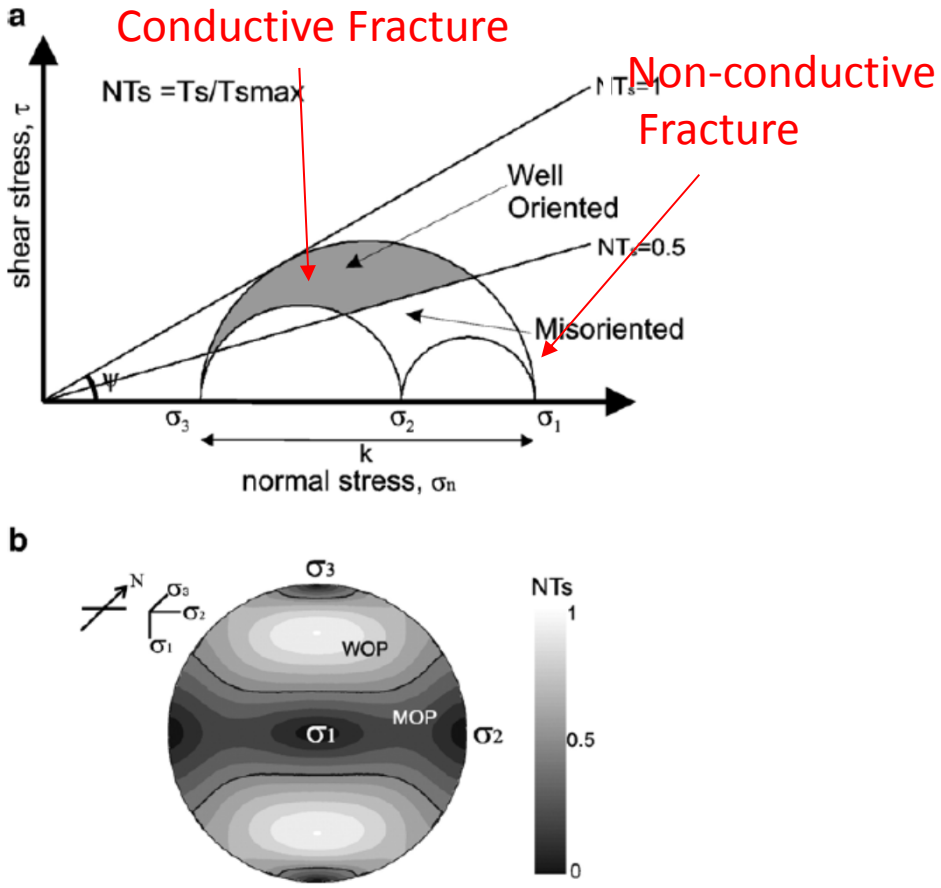

(Collettini and Trippetta, 2007)

Stress Assessment from Boreholes

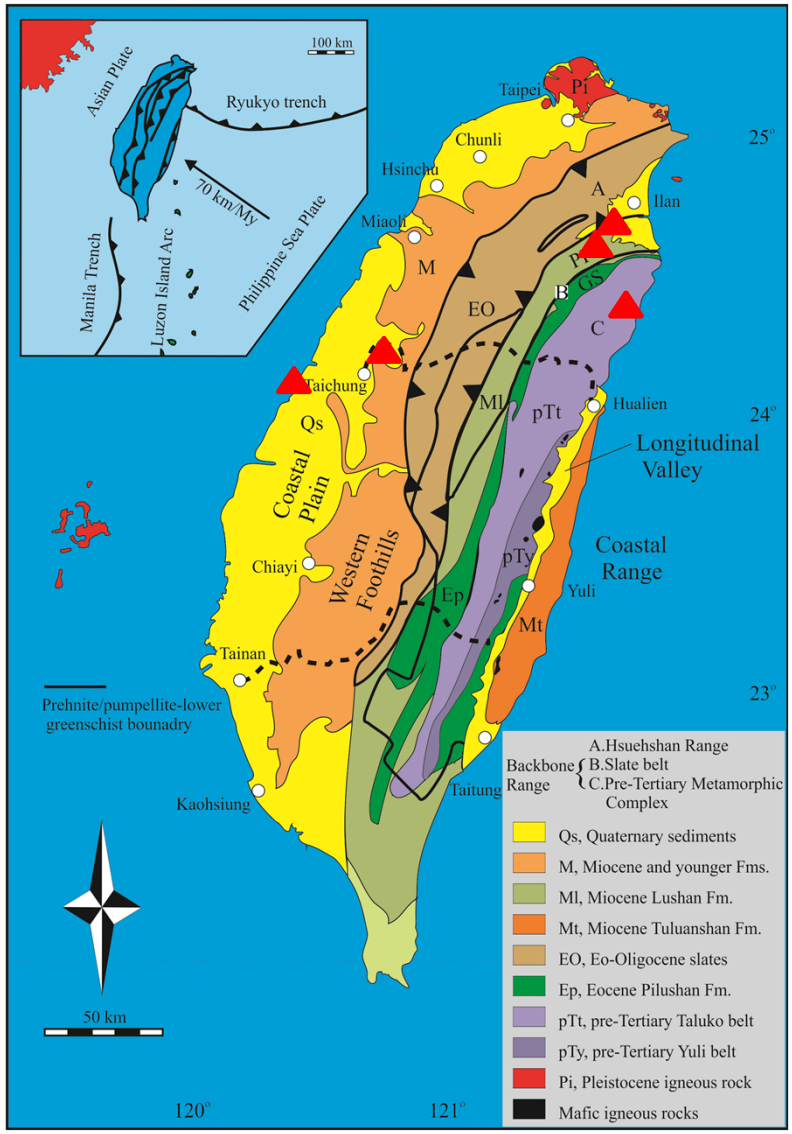

- CCS:~3000m, ASR, BO, HF
- TCDP:~1300m, ASR, BO, FM
- Waste:~600m, ASR, FS, FM
- Geotherm:600-800m, ASR, FS, FM, Vein
- Geotherm: 0-2200, ASR, HF, FM, DIFTs

CCS

Age		Martini's (1971) Zones	TPCS-M1井鑽遇之超微化石帶	TPCS-M1井鑽遇之地層
Pleistocene	Late	NN20	*G. oceanica* Zone	頭嵙山層
	Early	NN19	*P. lacunosa* Zone: *P. lacunosa* Subzone; small *Gephyrocapsa* Subzone; *C. dornicoides* Subzone NF-3	
Pliocene	Late	NN17-NN18	*C. macintyrei* Zone NF-77	1717 卓蘭層(418m)
		NN16	*Reticulofenestra minutula* Zone NF-246	2135 錦水頁岩(166m)
	Early	NN15 NN14 NN13	*Sphenoliths abies* Zone NF-274	2295 桂竹林層(117m)
		NN12		
Miocene	Late	NN11		
	Middle	NN10 NN9 NN8 NN7		
		NN6	*Cy. floridanus* Zone NF-325	觀音山砂岩(158m) 2450
		NN5	*S.heteromorphus* Zone NF-361	打鹿頁岩上段(104m) 2608
	Early	NN4	*H. ampliaperta* Zone NF-404	打鹿砂岩 (48m) 2712
		NN3	*S. belemnos* Zone NF-447	打鹿頁岩下段(40m) 2760 北寮層 井底3001.6m 2800
		NN2	*H. carteri* Zone	
		NN1		

(王明惠，未發表)

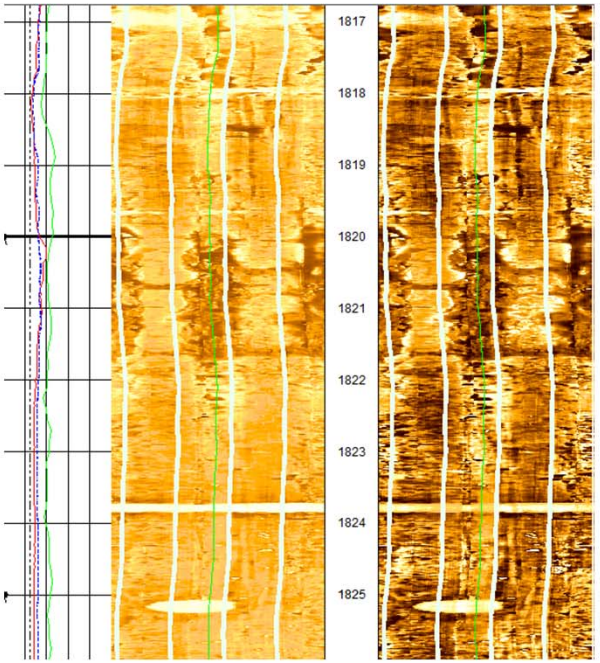

BO: 175.3+-9.1
WOB:42.2+-10.0

SHmax: 85.3+-9.1 deg
Magnitude: ??

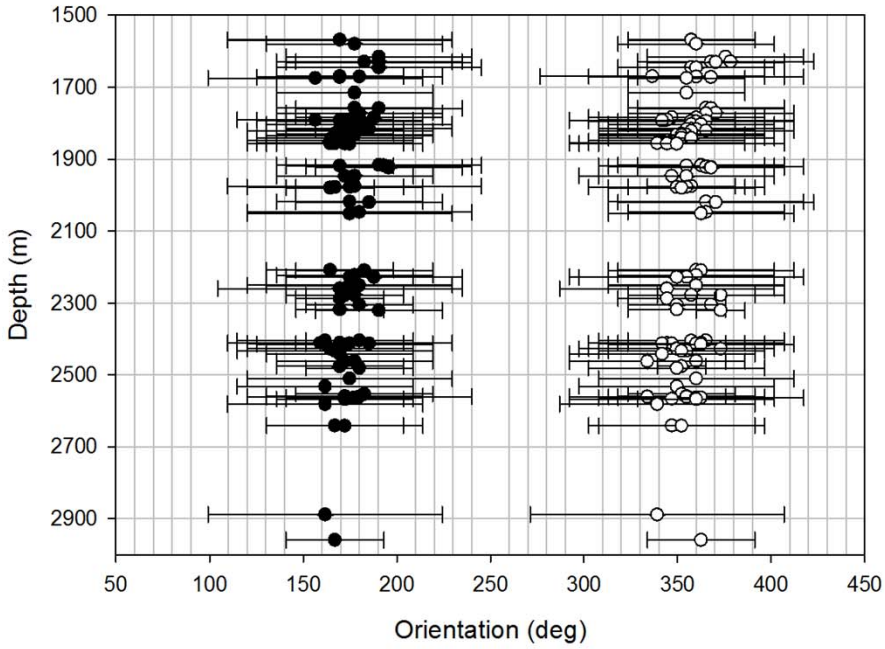

Stress_Depth

ASR

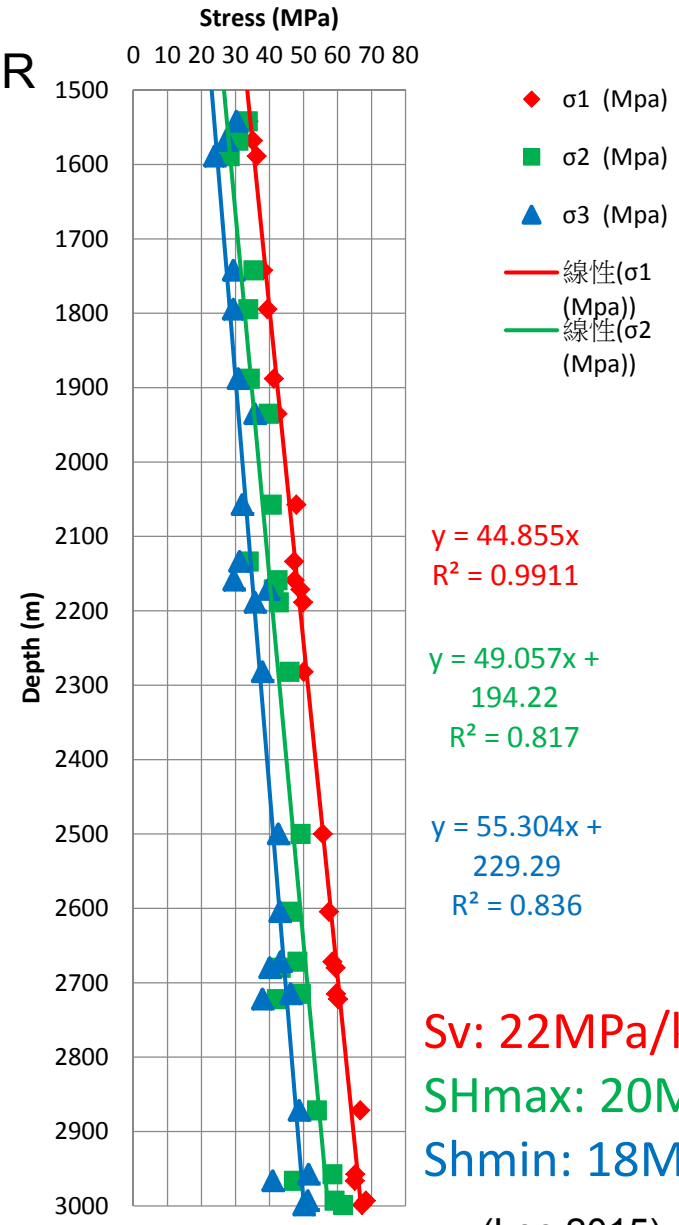

y = 44.855x
R^2 = 0.9911

y = 49.057x + 194.22
R^2 = 0.817

y = 55.304x + 229.29
R^2 = 0.836

Sv: 22MPa/km

SHmax: 20MPa/km

Shmin: 18MPa/km

(Lee 2015)

HF

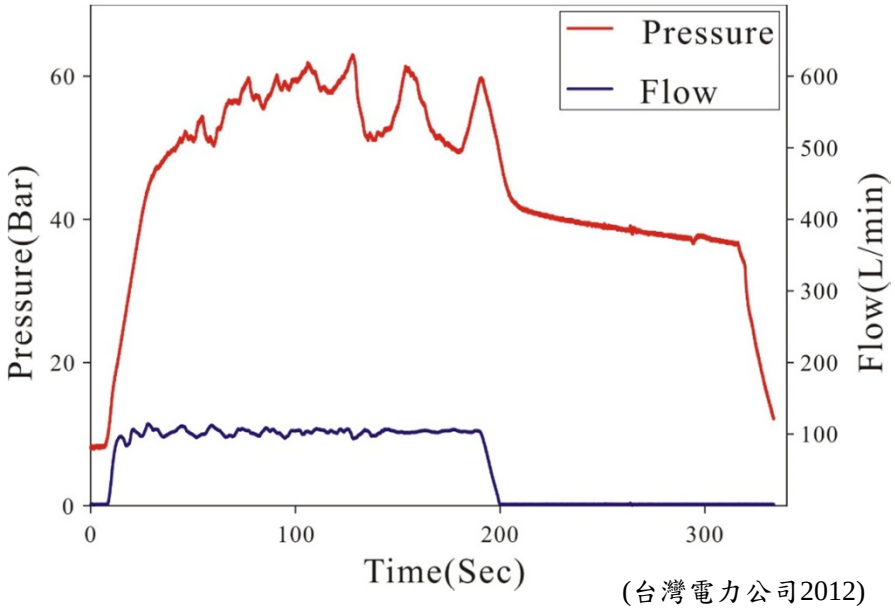

(台灣電力公司2012)

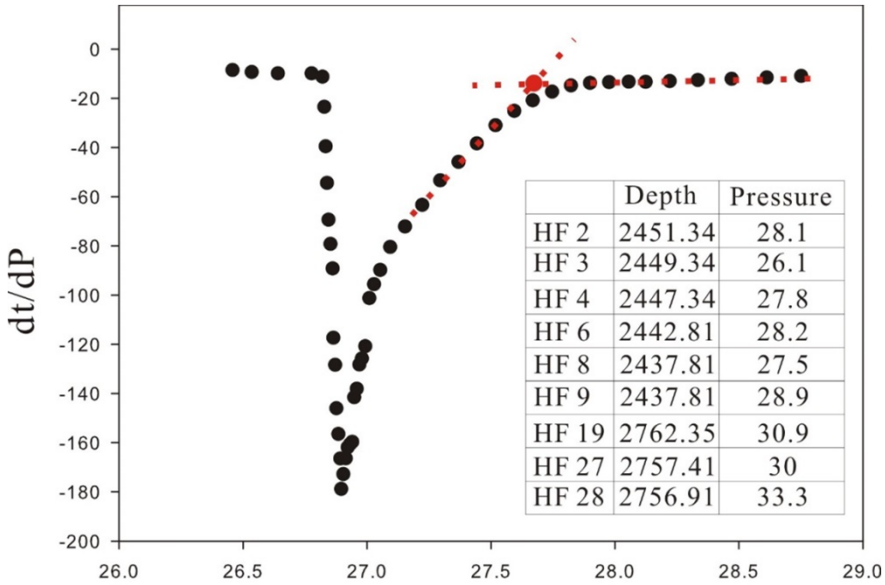

	Depth	Pressure
HF 2	2451.34	28.1
HF 3	2449.34	26.1
HF 4	2447.34	27.8
HF 6	2442.81	28.2
HF 8	2437.81	27.5
HF 9	2437.81	28.9
HF 19	2762.35	30.9
HF 27	2757.41	30
HF 28	2756.91	33.3

(Cheng et al., 2016)

Taiwan Chelungpu-fault Drilling Project (TCDP)

ASR

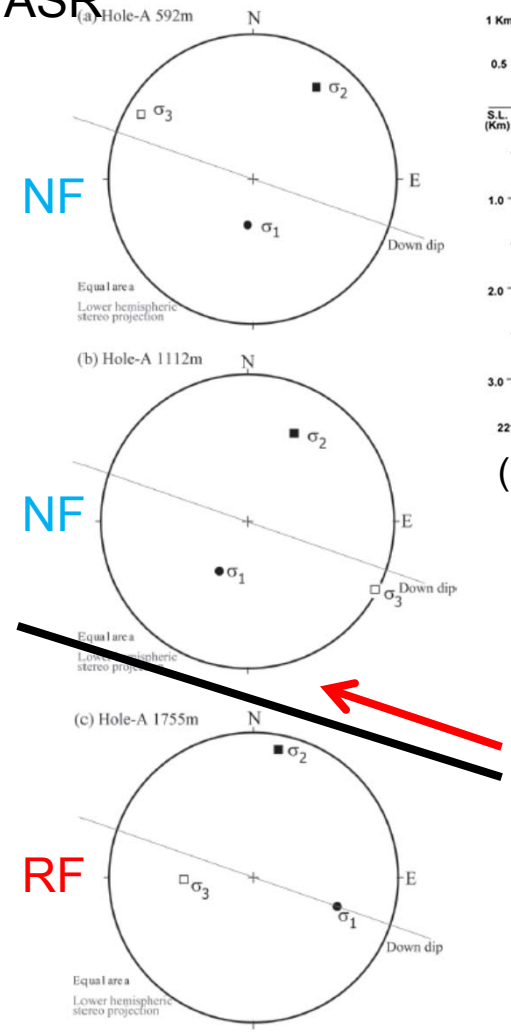

(Lin et al., 2007)

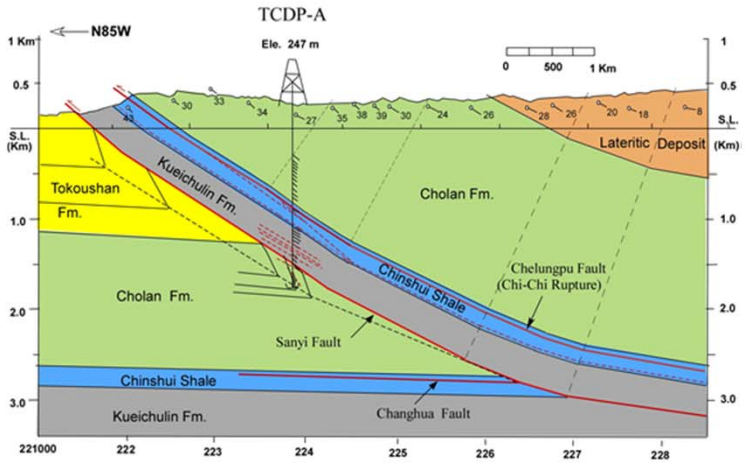

(Hung et al., 2007)

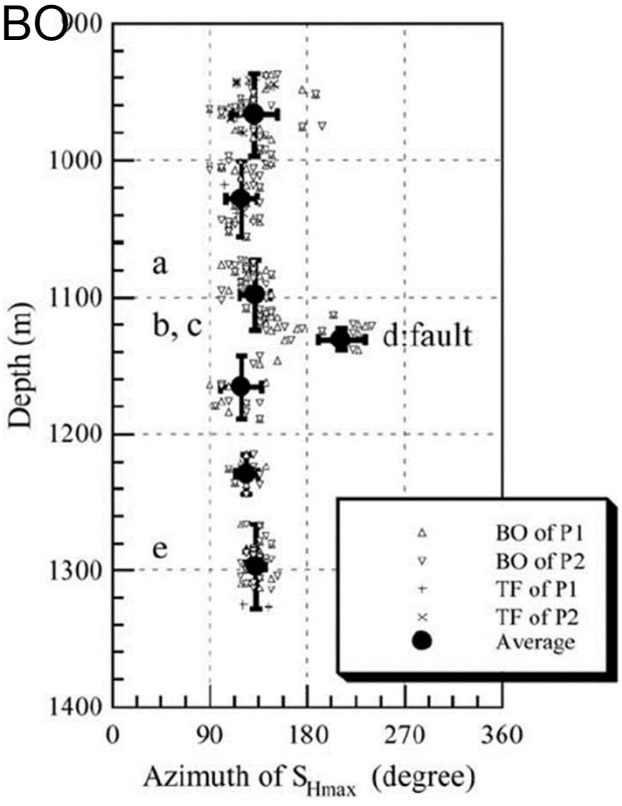

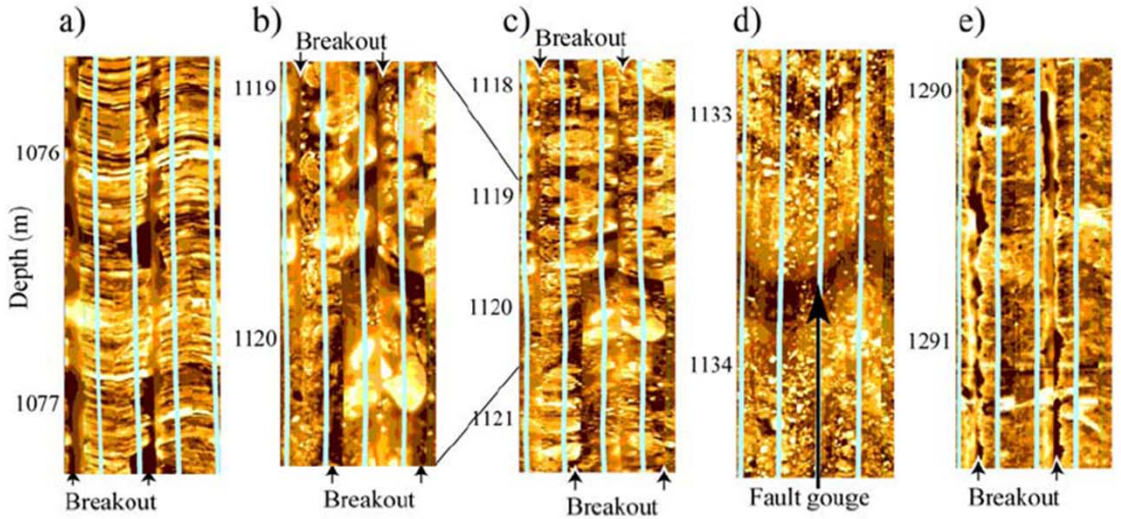

(Lin et al., 2006)

HF

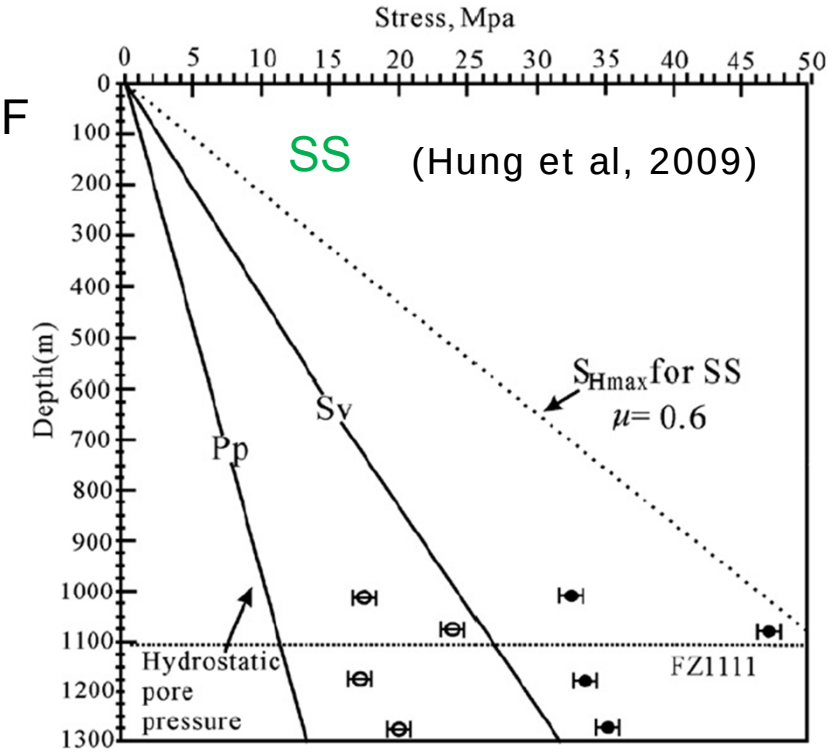

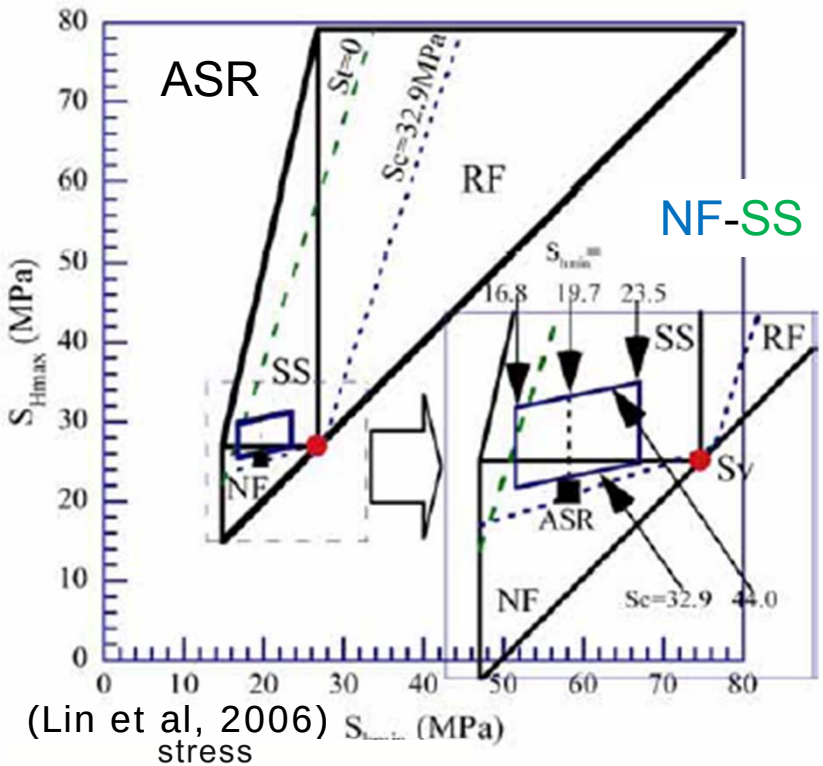

AE

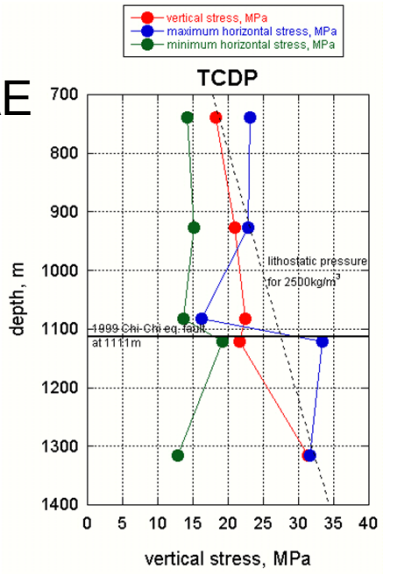

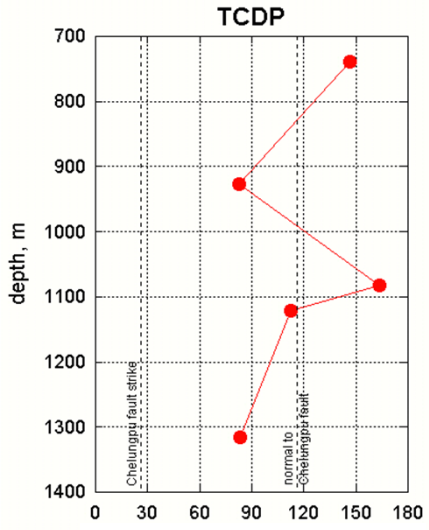

(Yabe et al., 2008)

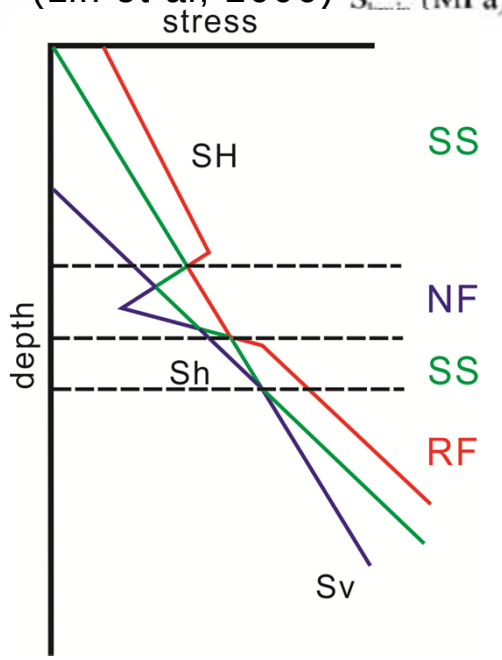

FM

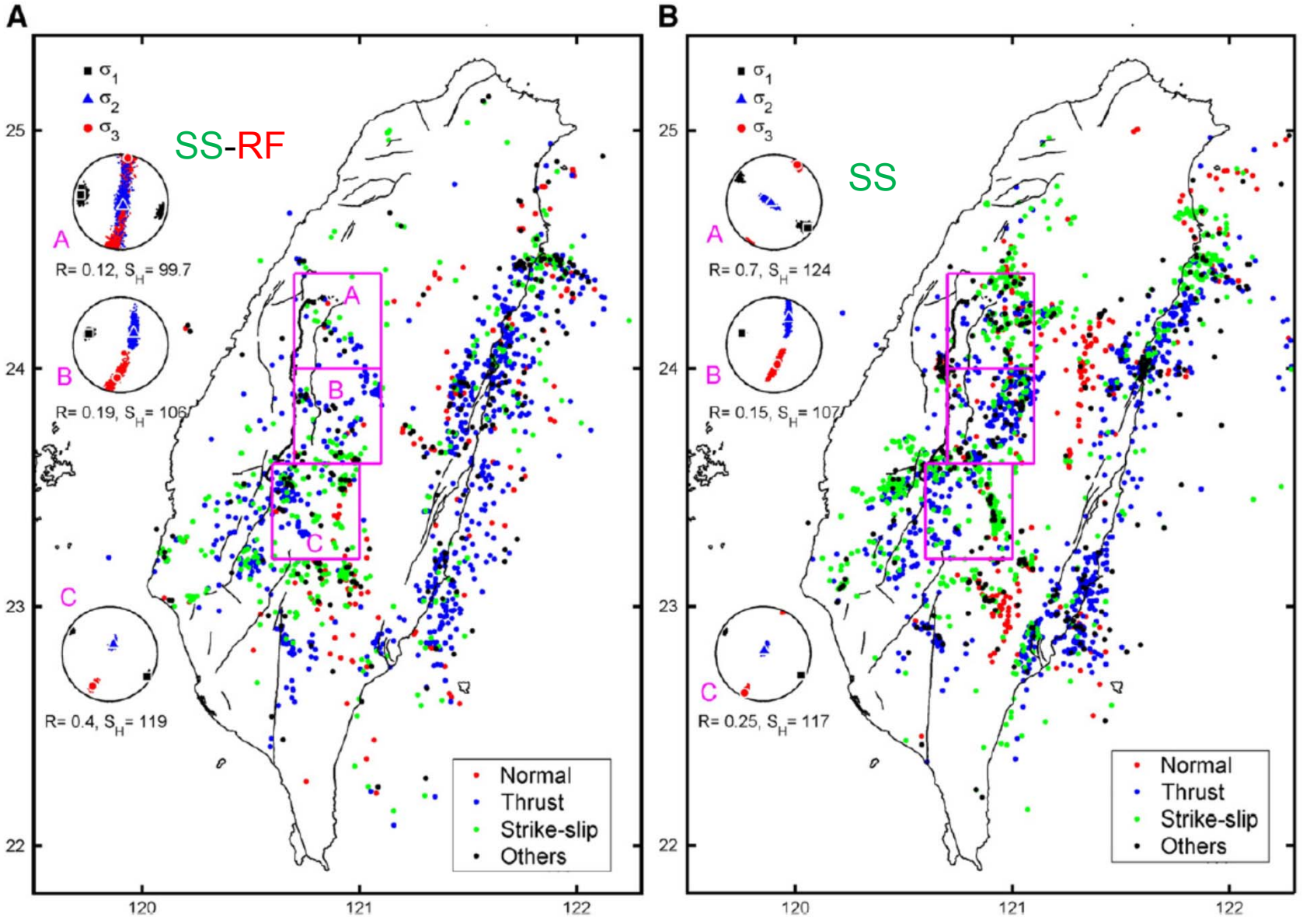

(Wu et al., 2010)

FS

Inter-seismic

Co-seismic

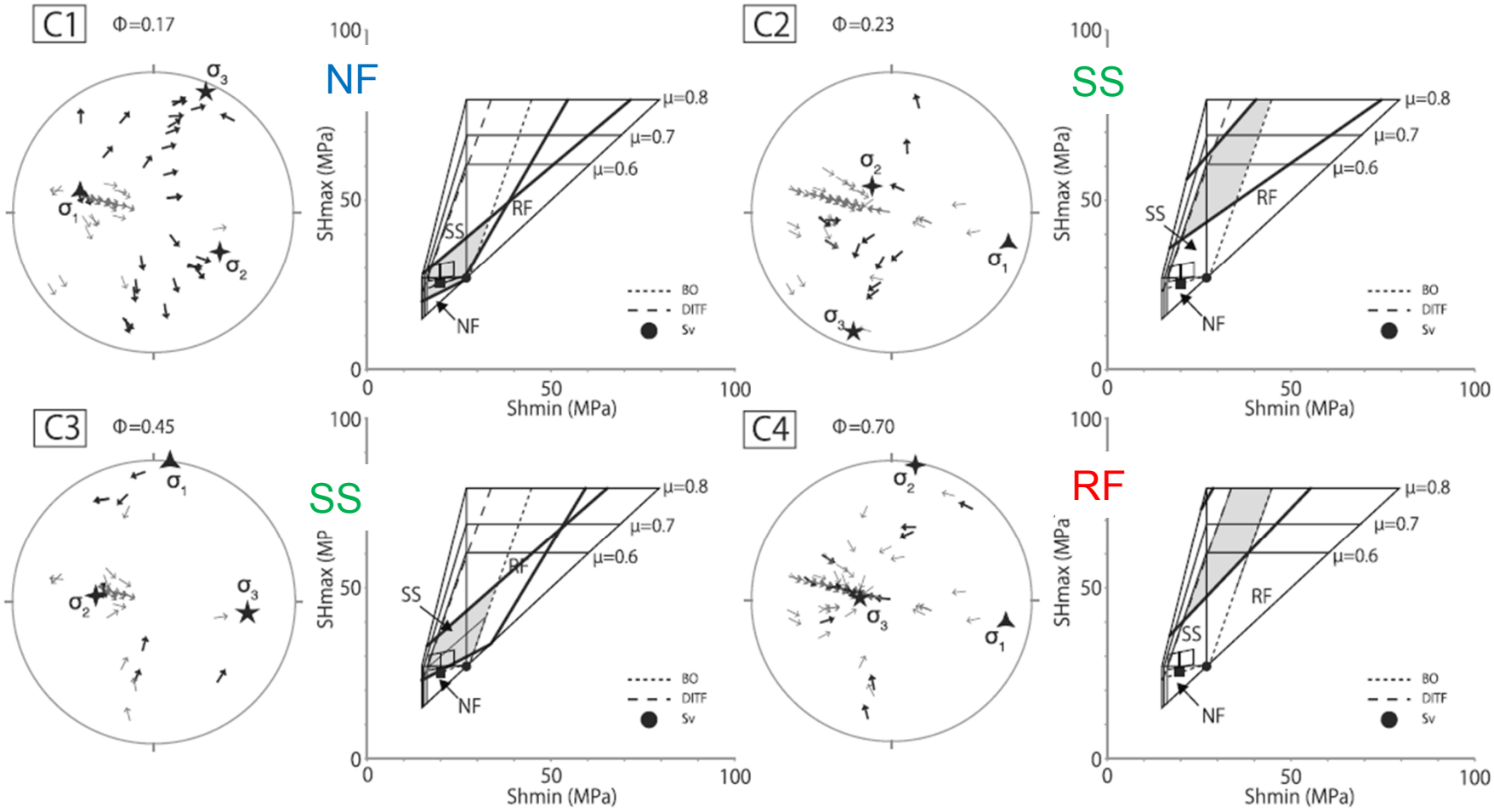

(Hashimoto et al., 2015)

Waste Disposal, Metagranite, Hoping

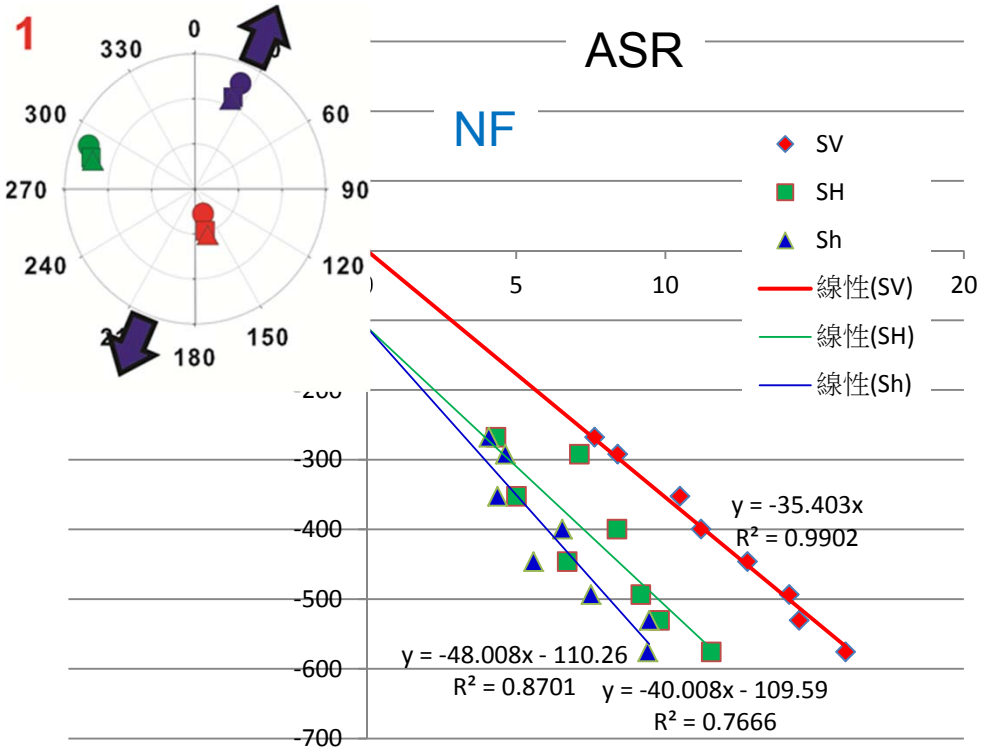

(Li, 2015)

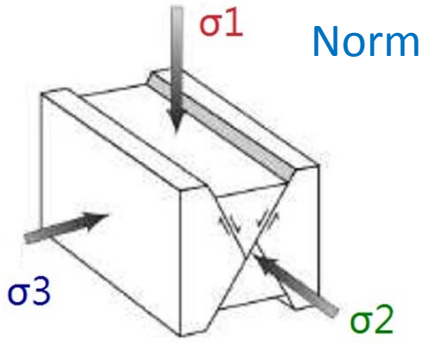

Normal Faulting

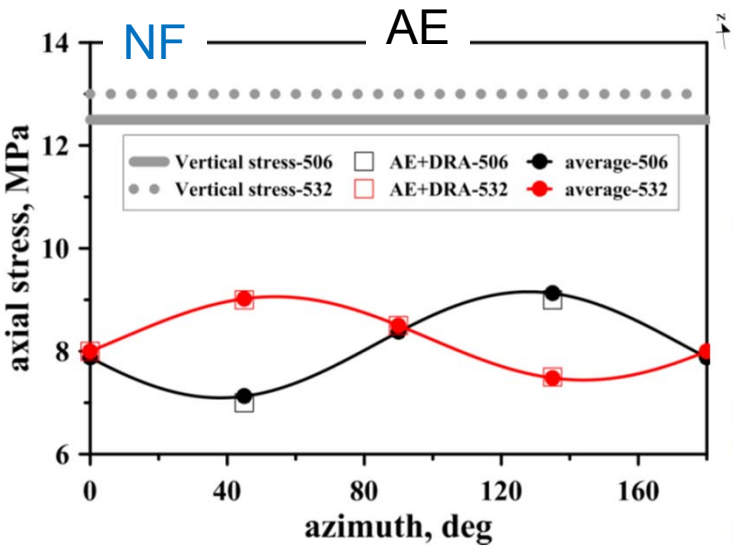

(Pan et al., 2013)

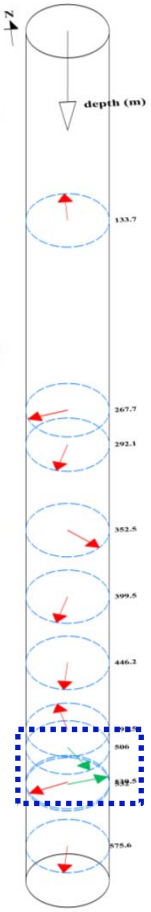

Sv: 26MPa/km

SHmax: 22MPa/km

Shmin: 19MPa/km

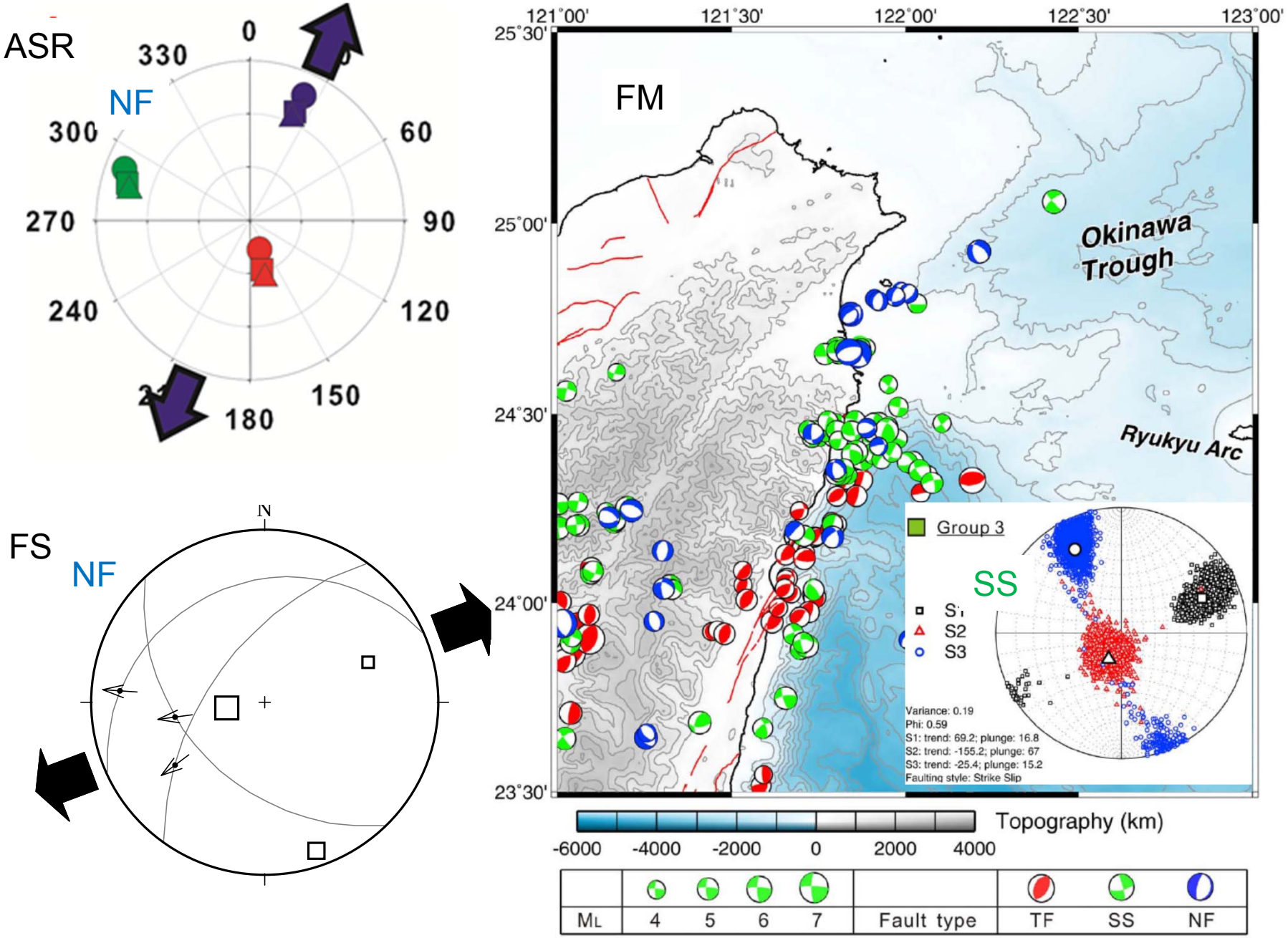

(Huang et al., 2012)

Open-Filling Fractures

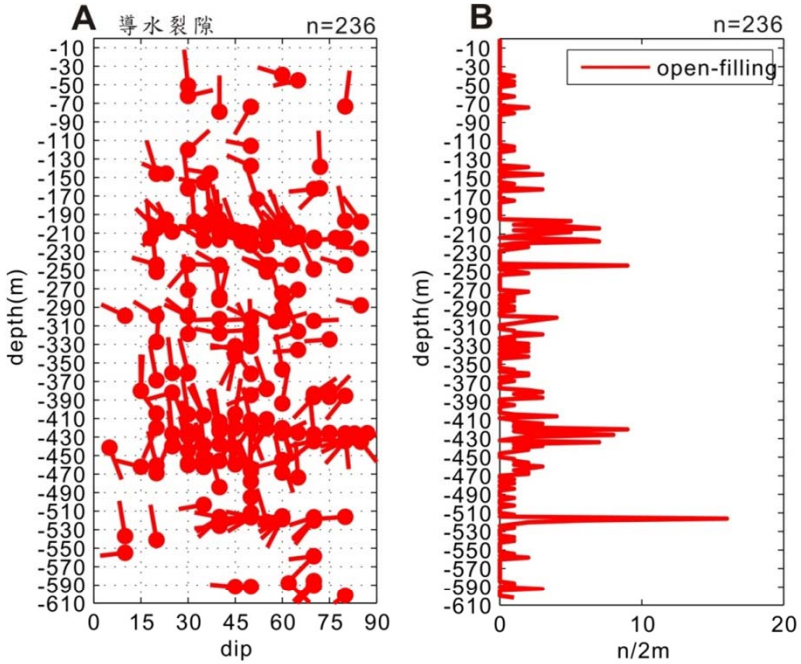

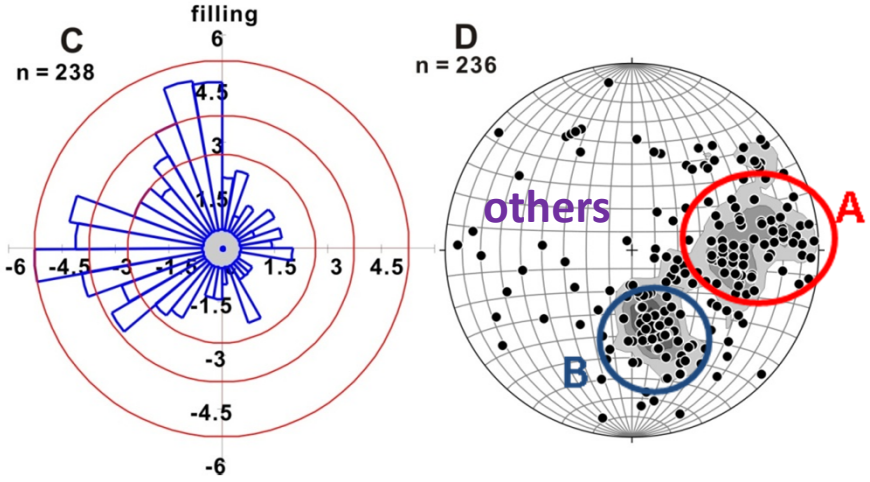

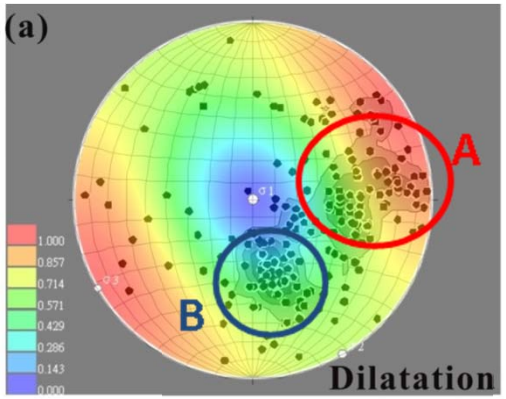

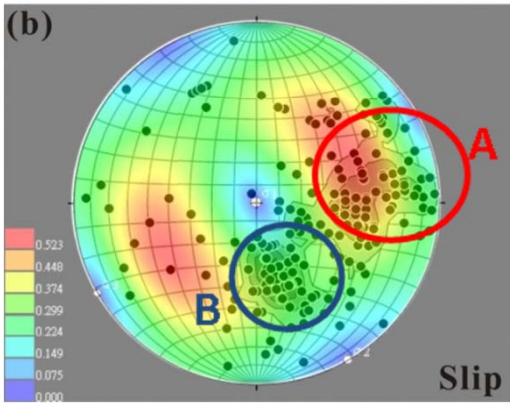

(Lin, 2015)

CingShui Geotherm, Ilan

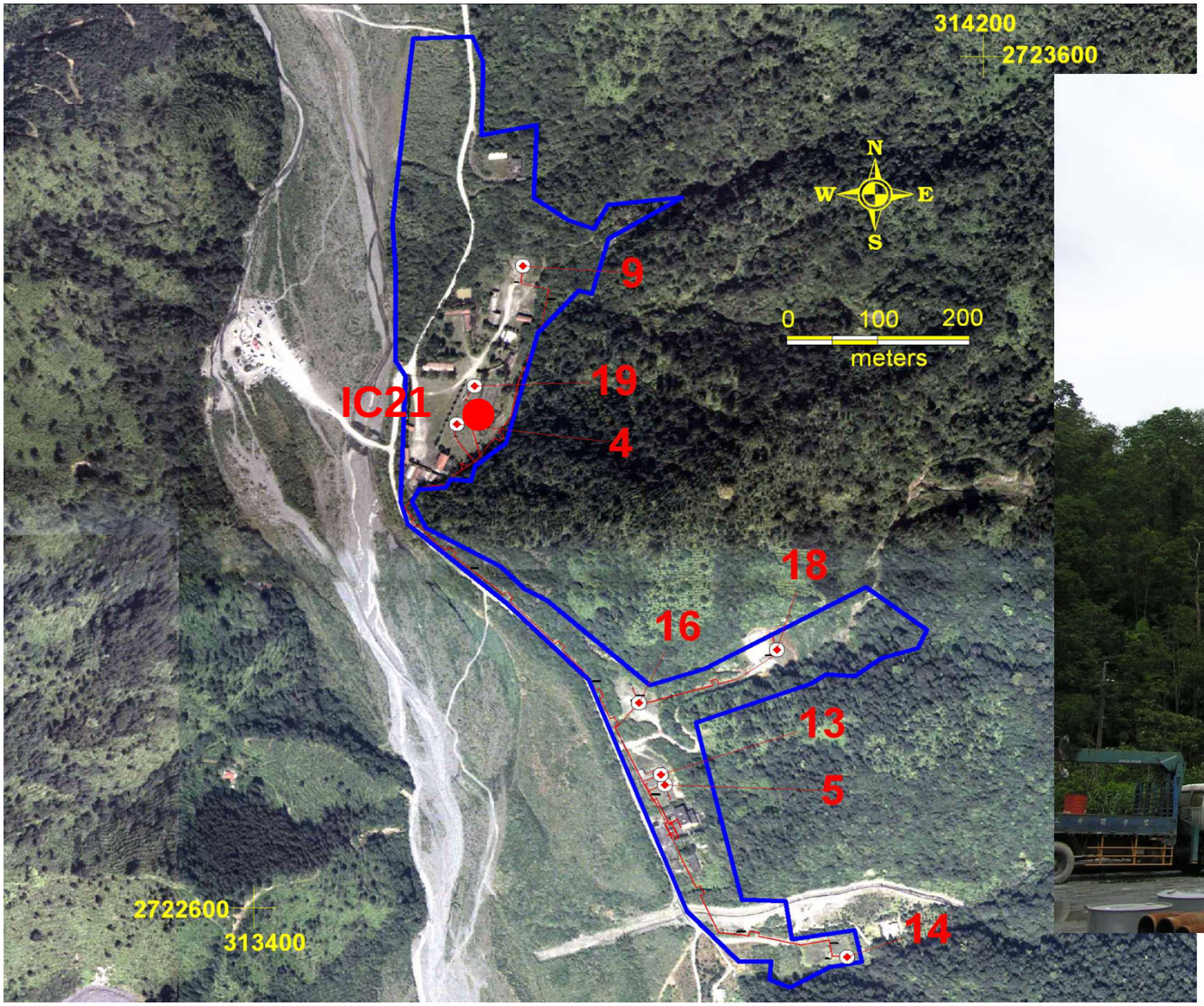

CingShui Geotherm, Ilan

FM

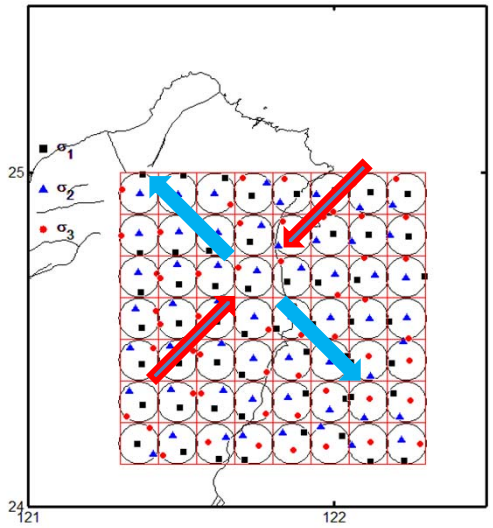

FS

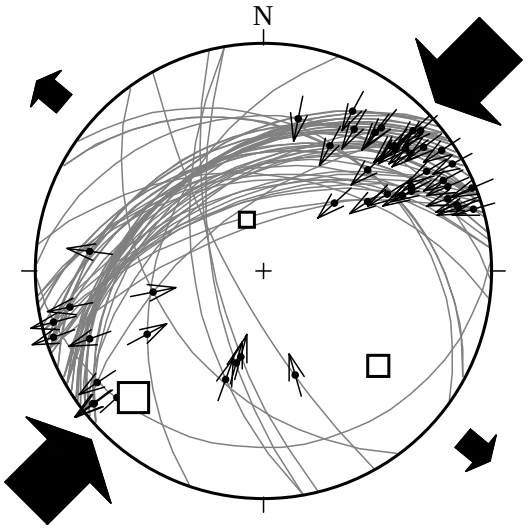

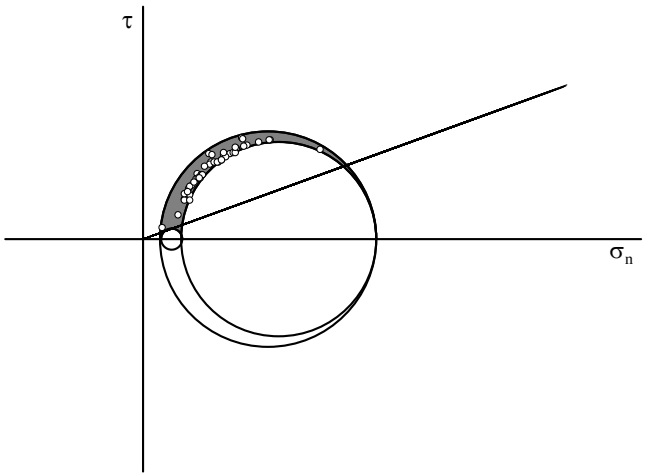

FS

σ_1

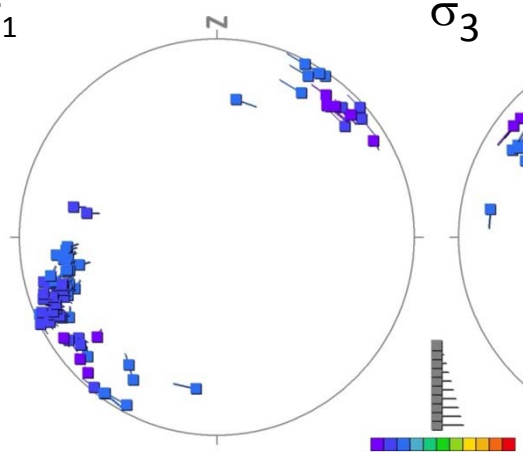

σ_3

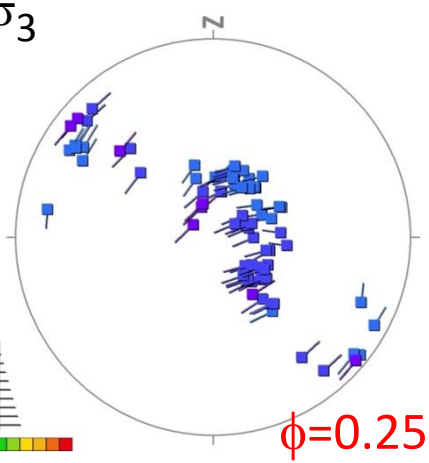

ϕ=0.25

ASR

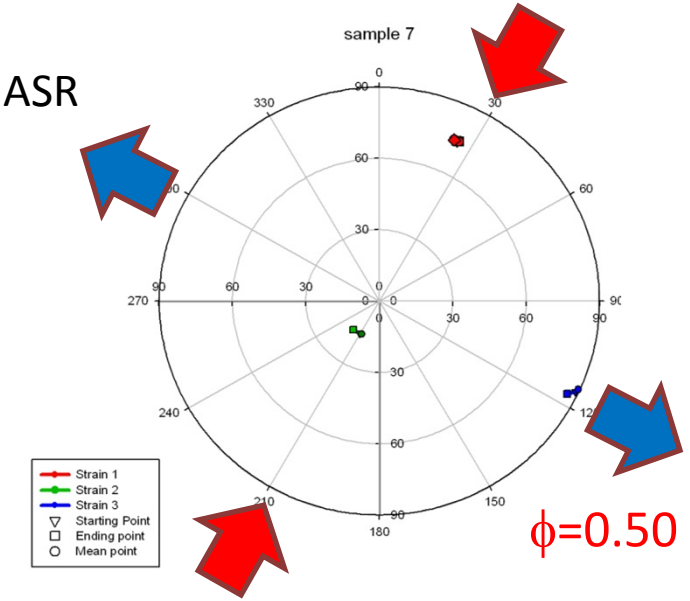

ϕ=0.50

Core Observation

vein, calcite, open

vein, calcite, close

kink, calcite, close

NoFilling vs Open Filling

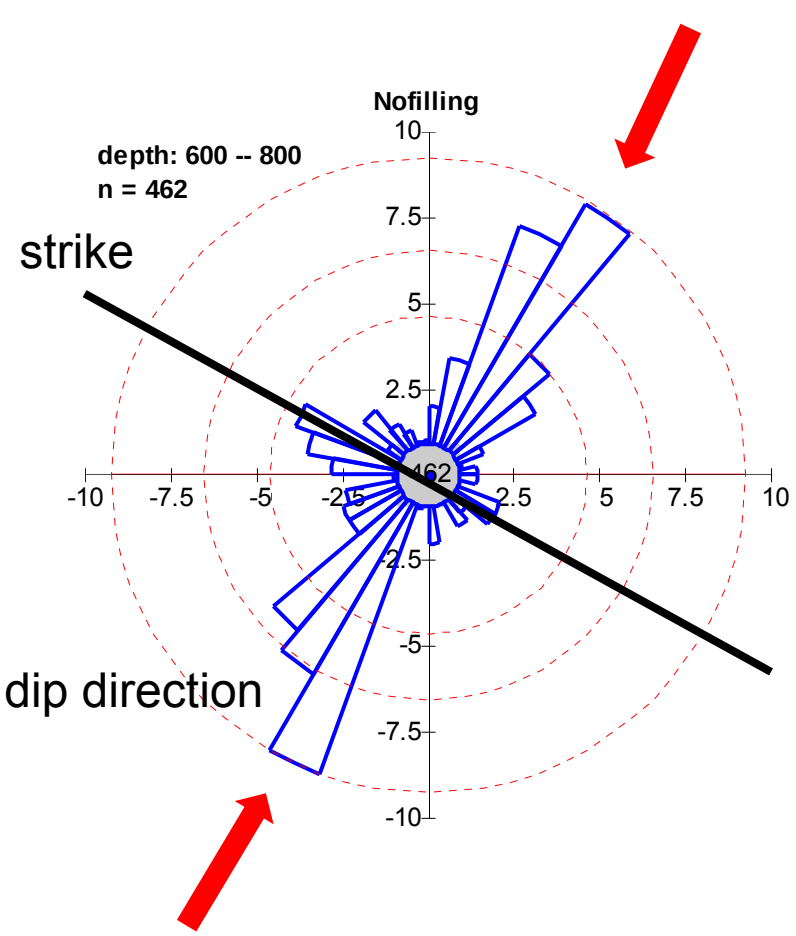

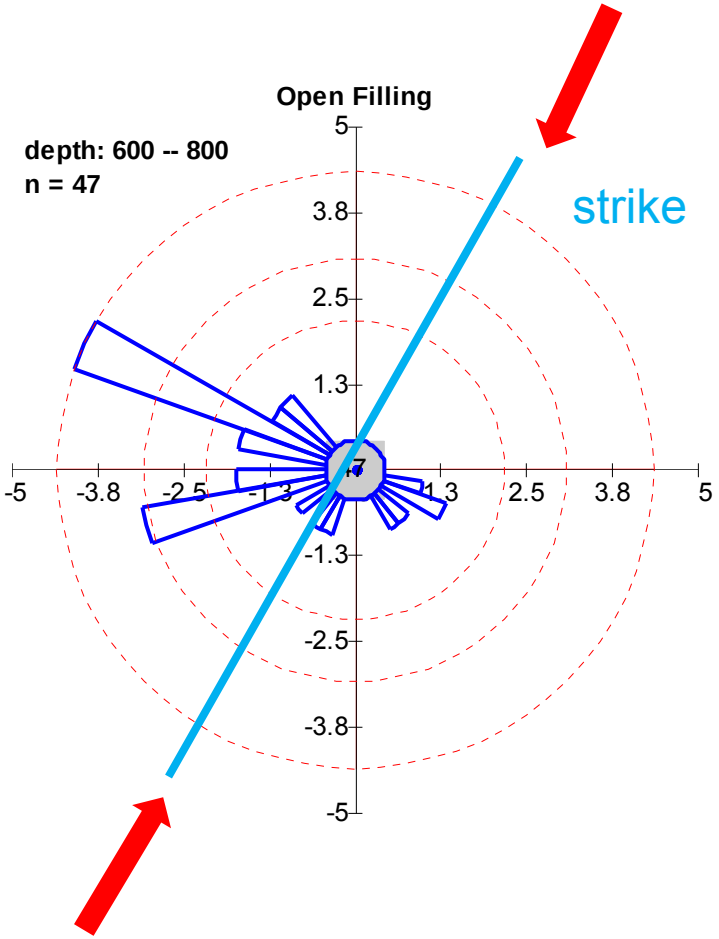

Hydraulic Fracturing

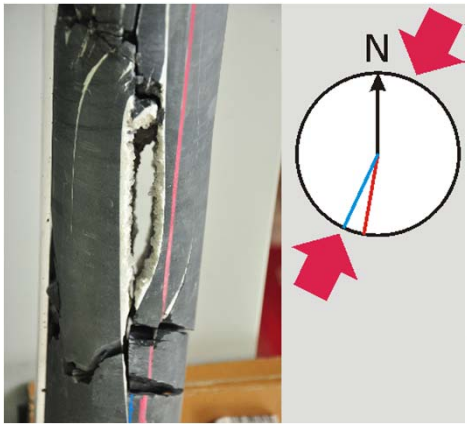

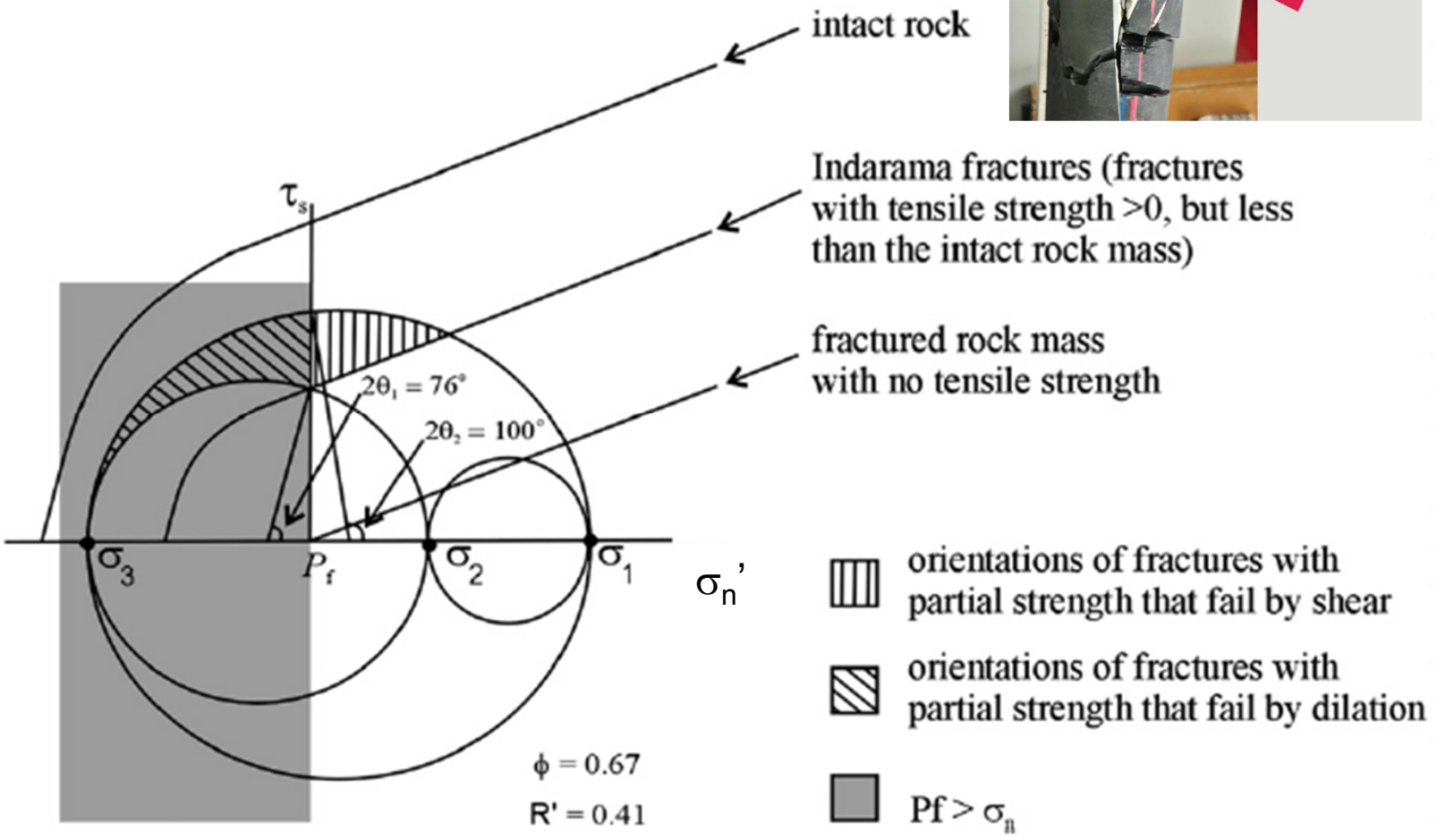

$Pf \geqq aT_0 + \sigma_3$

(McKeangey et al., 2004)

Stress-Vein Integration

Stereonet Mohr

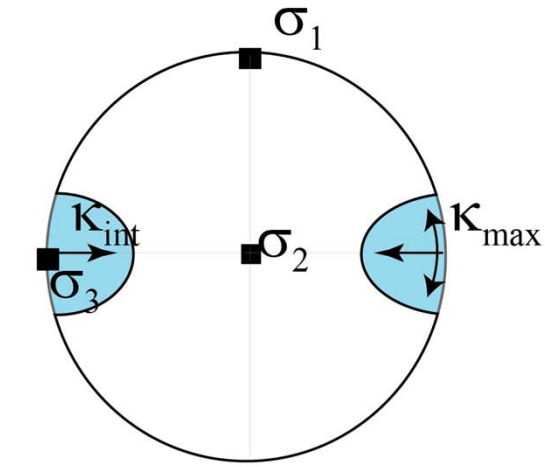

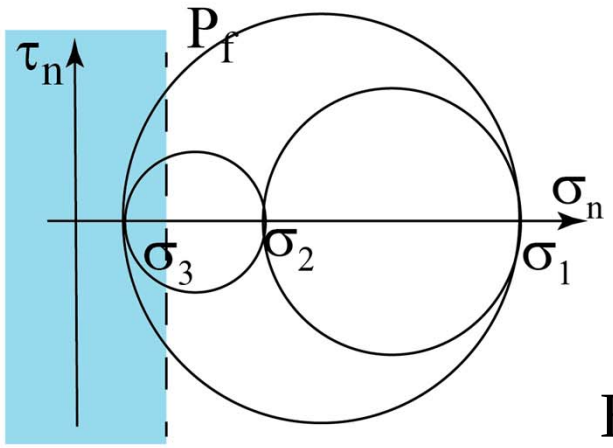

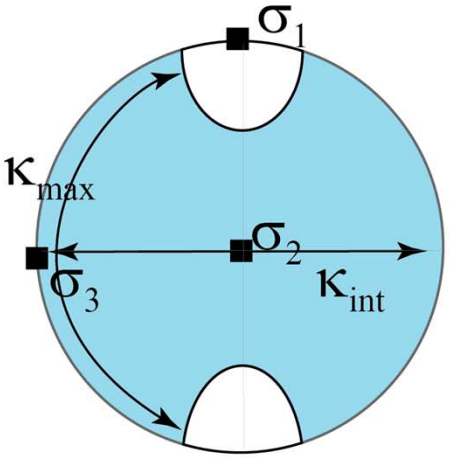

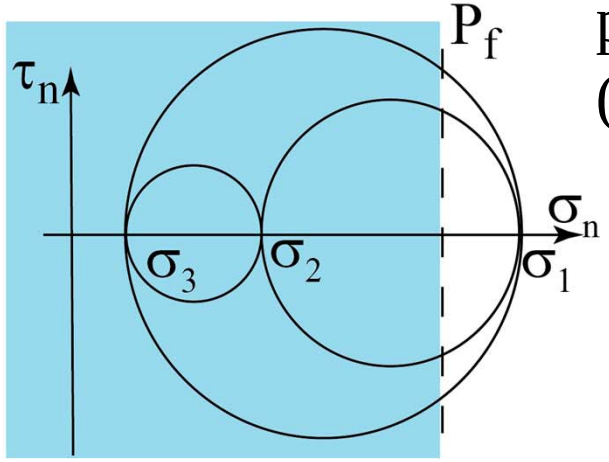

$$\Phi = \frac{\kappa_{int}}{\kappa_{max}} = \frac{\sigma_2 - \sigma_3}{\sigma_1 - \sigma_3}$$

Bingham concentration parameter

$(\kappa_{max} \leqq \kappa_{int} \leqq 0)$

(Jolly & Sanderson, 1997; Yamaji et al., 2010)

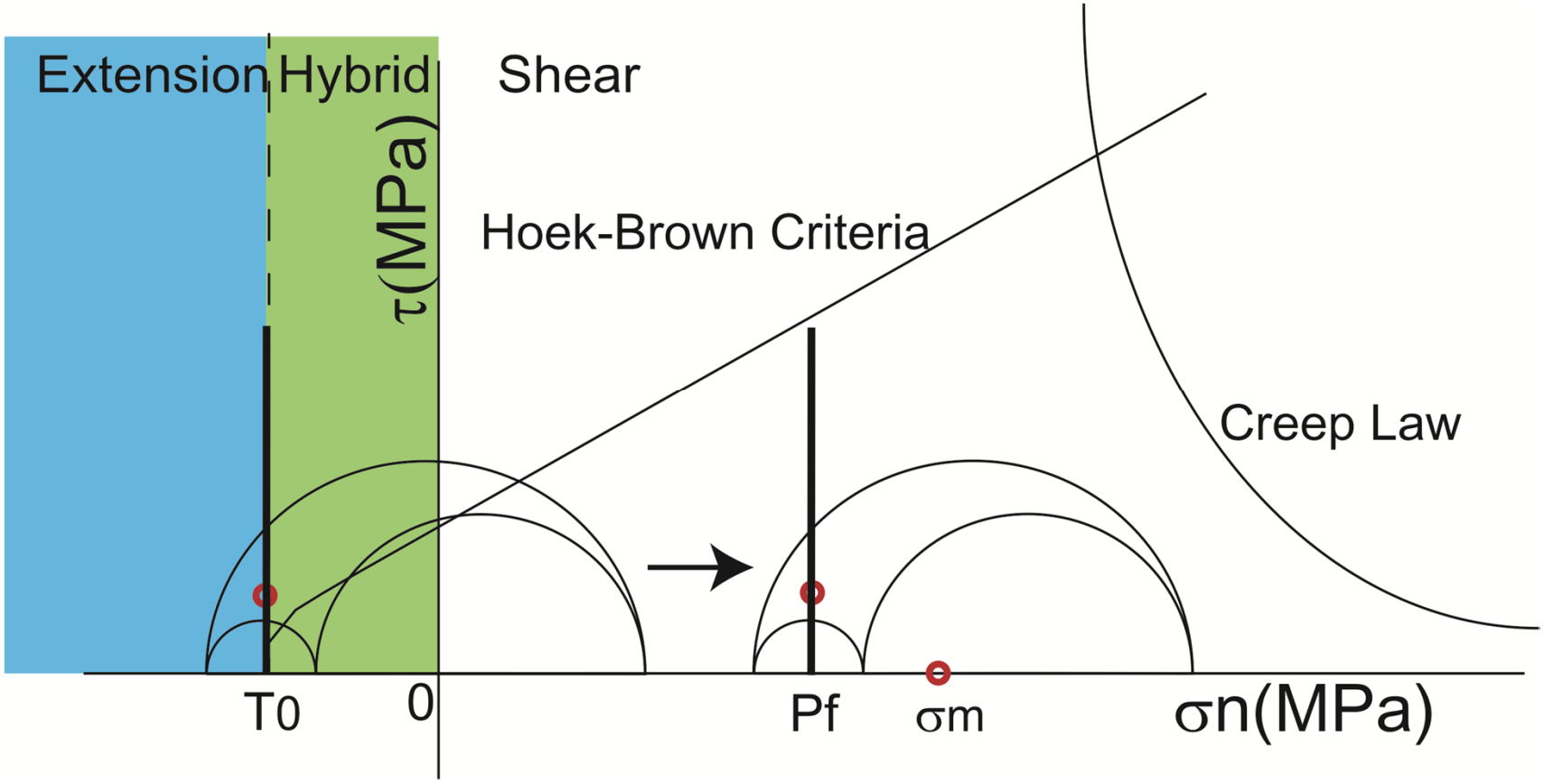
Extension
Hybrid
Shear
τ(MPa)
Hoek-Brown Criteria
Creep Law
T0
0
Pf
σm
σn(MPa)

SanHsin Geotherm, Ilan

SanHsin

HF

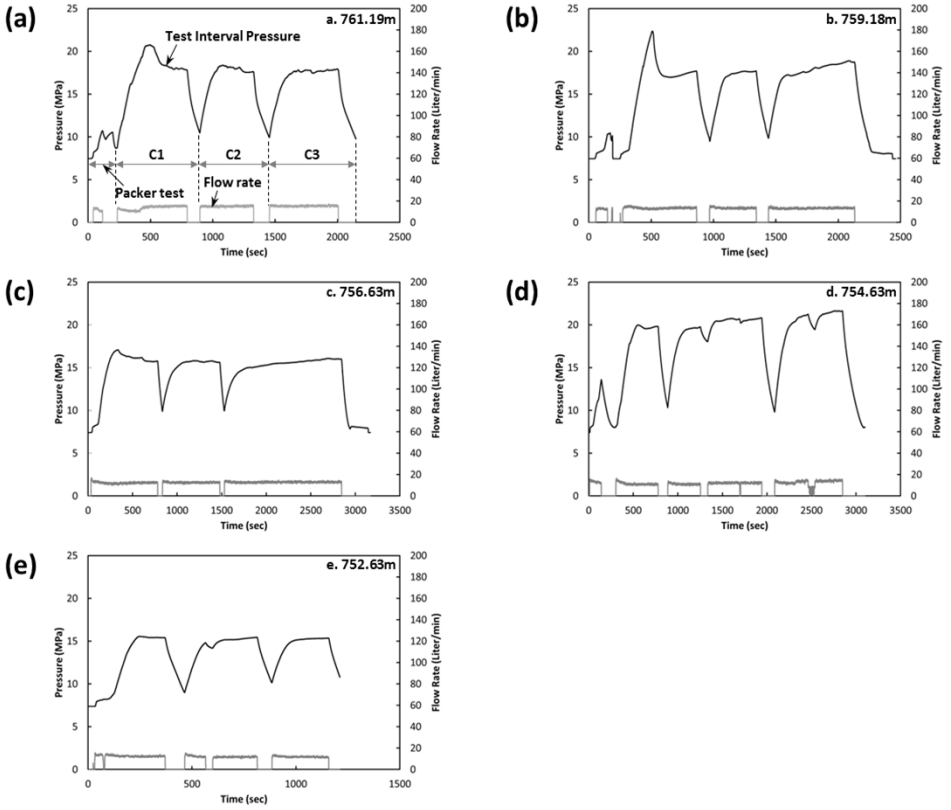

Shmin~13.6MPa @ 750-765m

DCDA

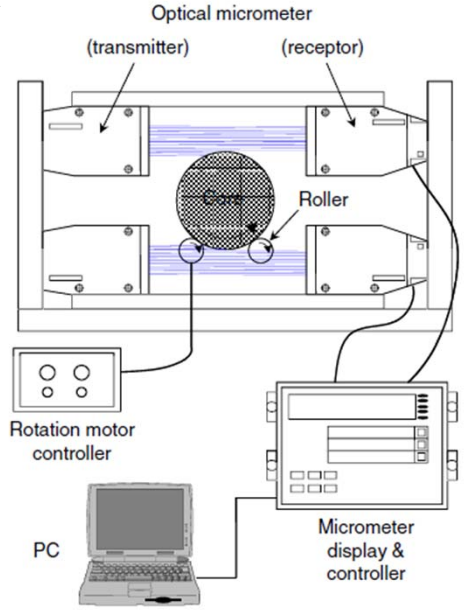

SHmin-Shmin~23-27MPa @734m

Stress Magnitude

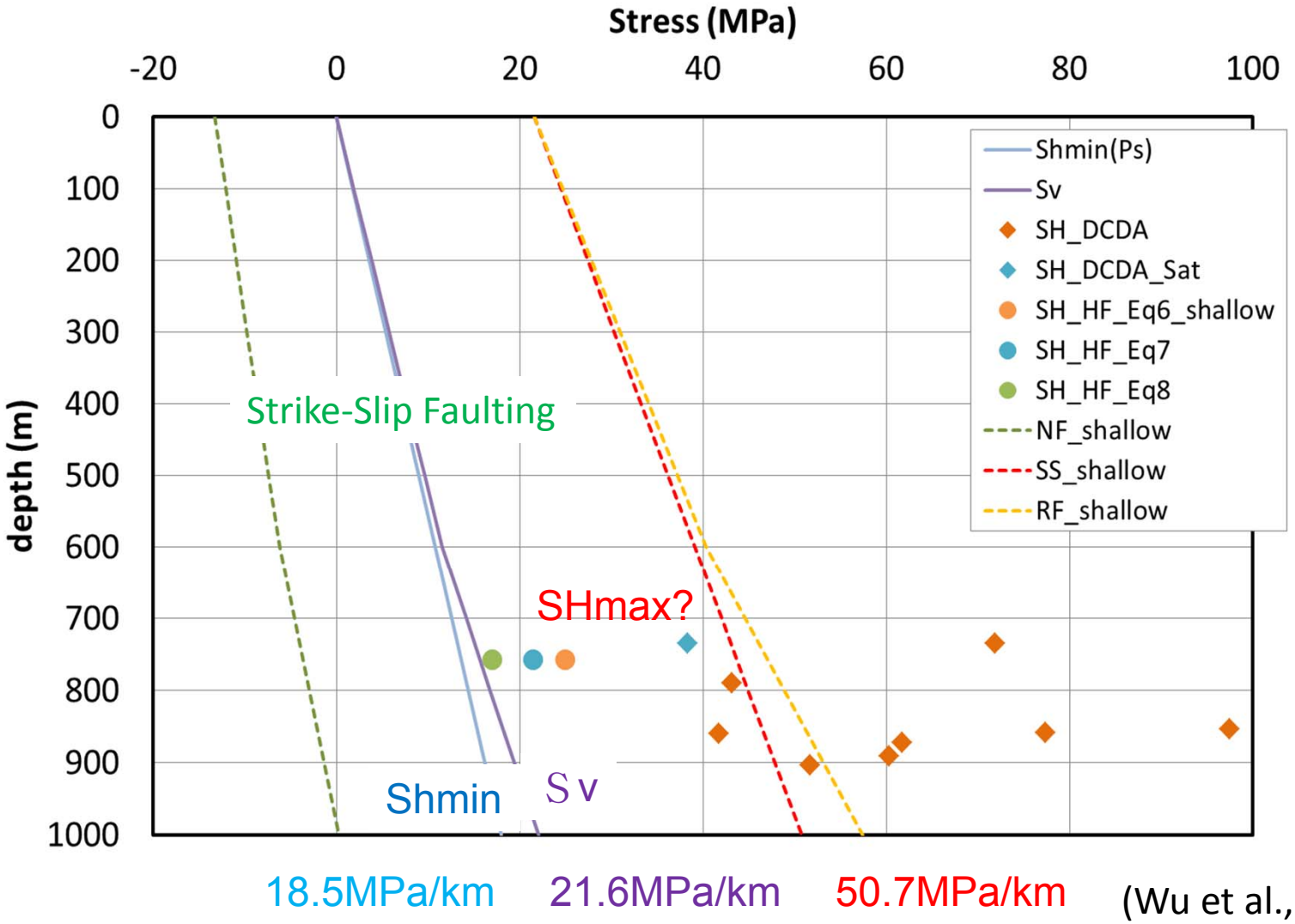

(Wu et al., 2015)

JY-01

102-2

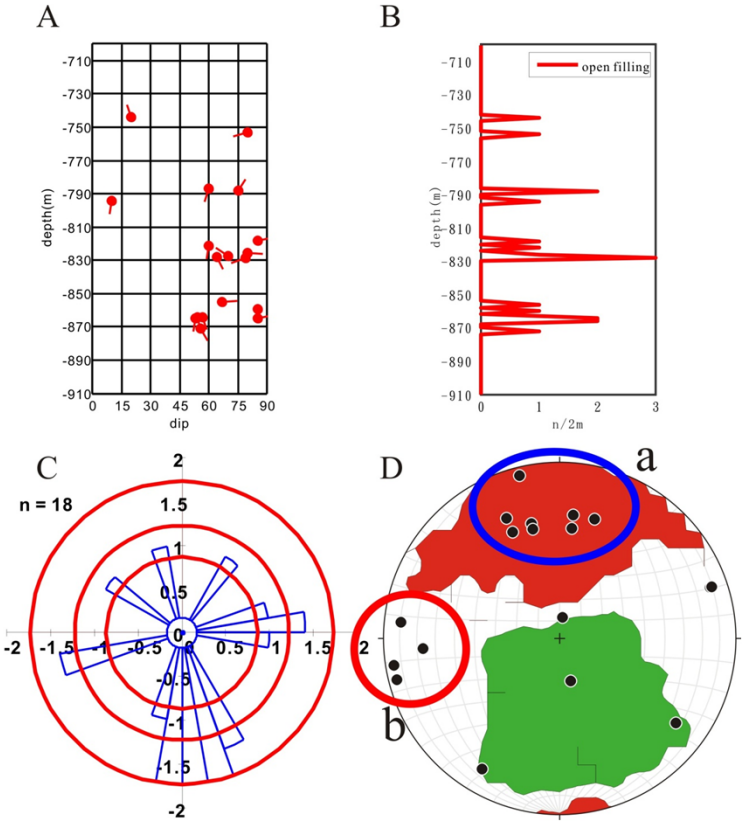

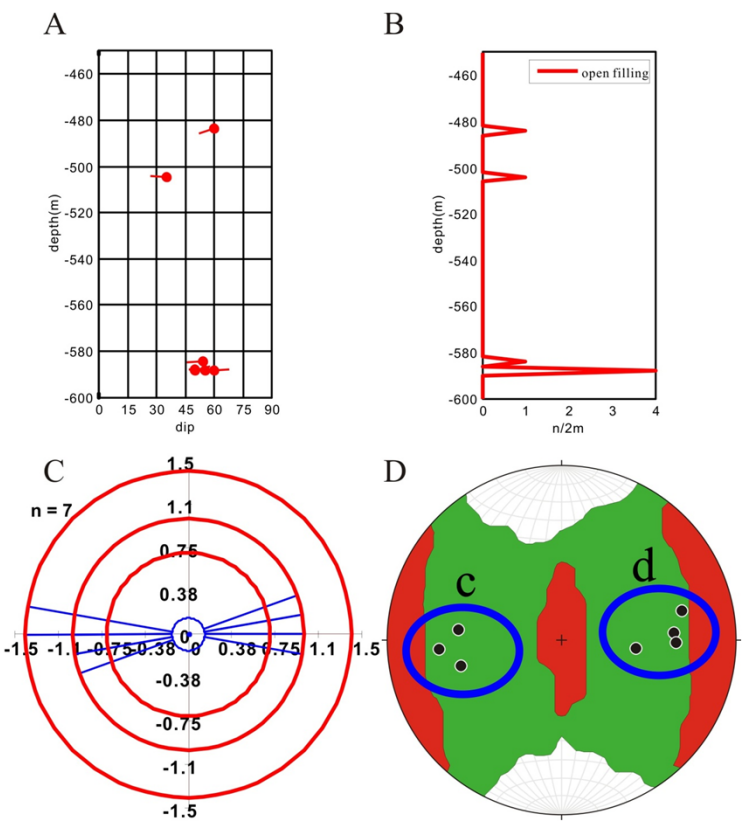

(Kao, 2016)

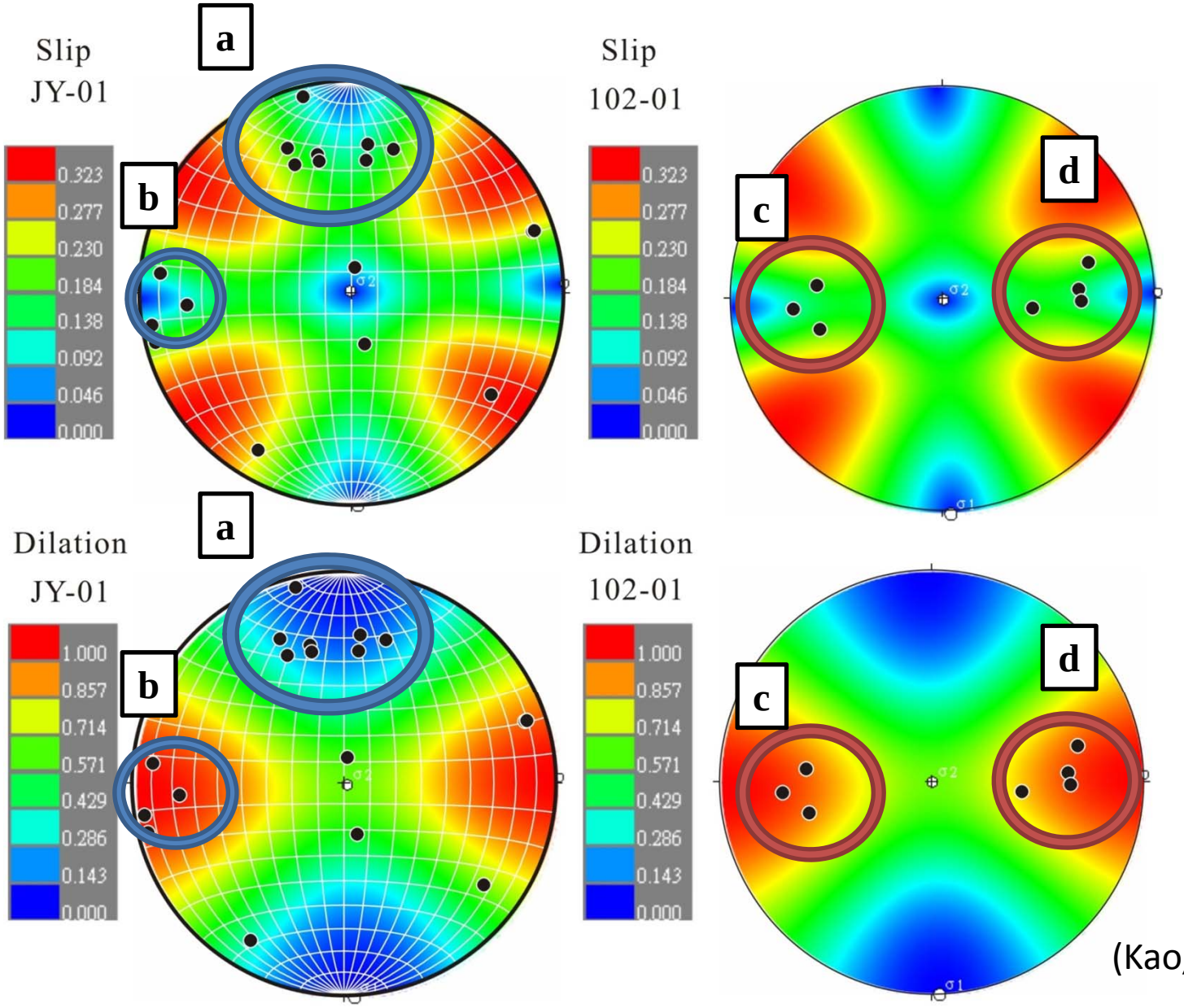
Slip
JY-01
a
b
0.323
0.277
0.230
0.184
0.138
0.092
0.046
0.000
Slip
102-01
c
d
0.323
0.277
0.230
0.184
0.138
0.092
0.046
0.000
Dilation
JY-01
a
b
1.000
0.857
0.714
0.571
0.429
0.286
0.143
0.000
Dilation
102-01
c
d
1.000
0.857
0.714
0.571
0.429
0.286
0.143
0.000

(Kao, 2016)

HCL-1

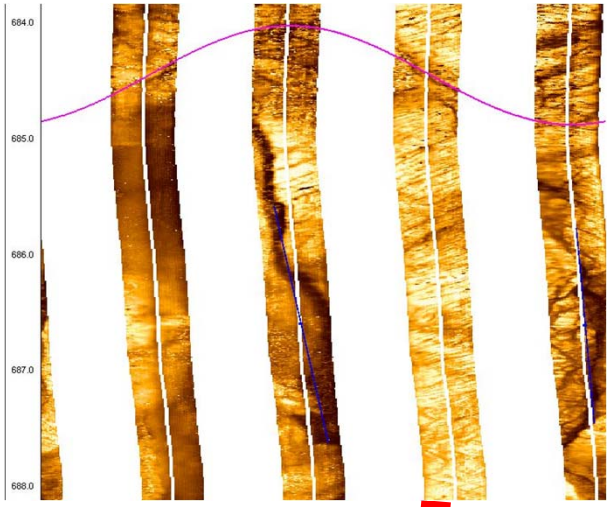

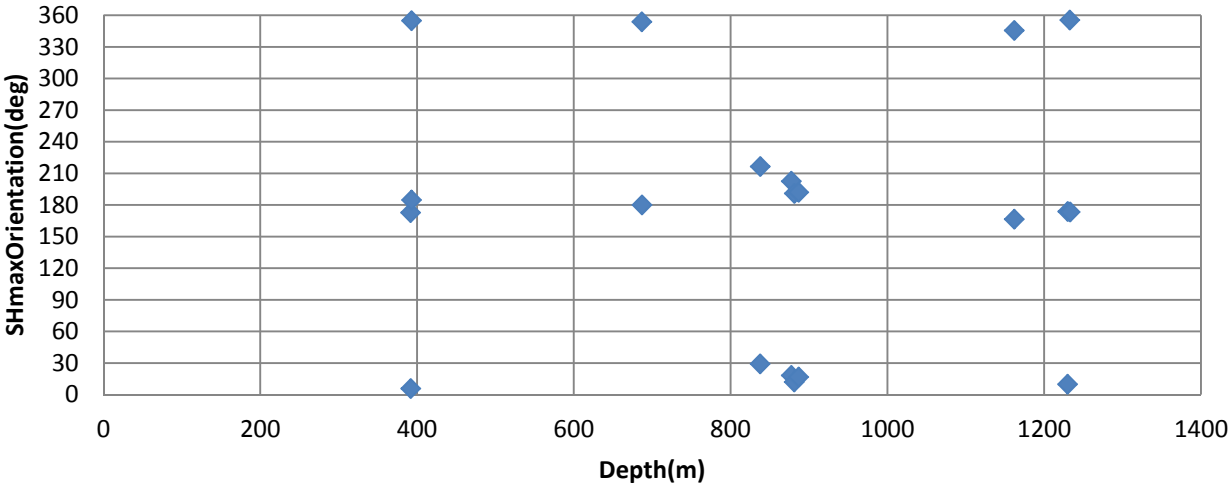

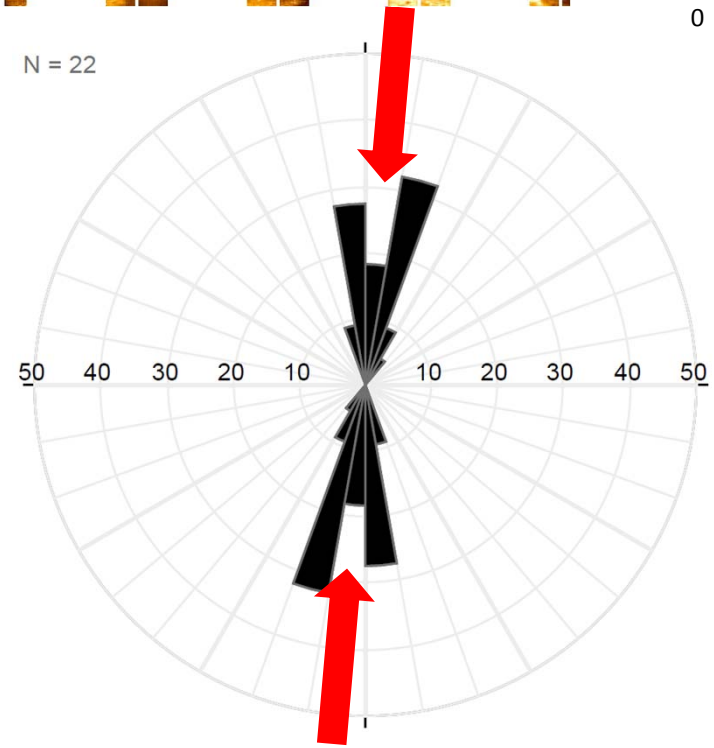

- SHmax orientation
- Mean Vector = 006.3° ± 05.9°; Average Length = 0.8948
- Circular Variance = 0.1052;
- kappa = 4.8587

以單軸抗壓強度&水破資料估計

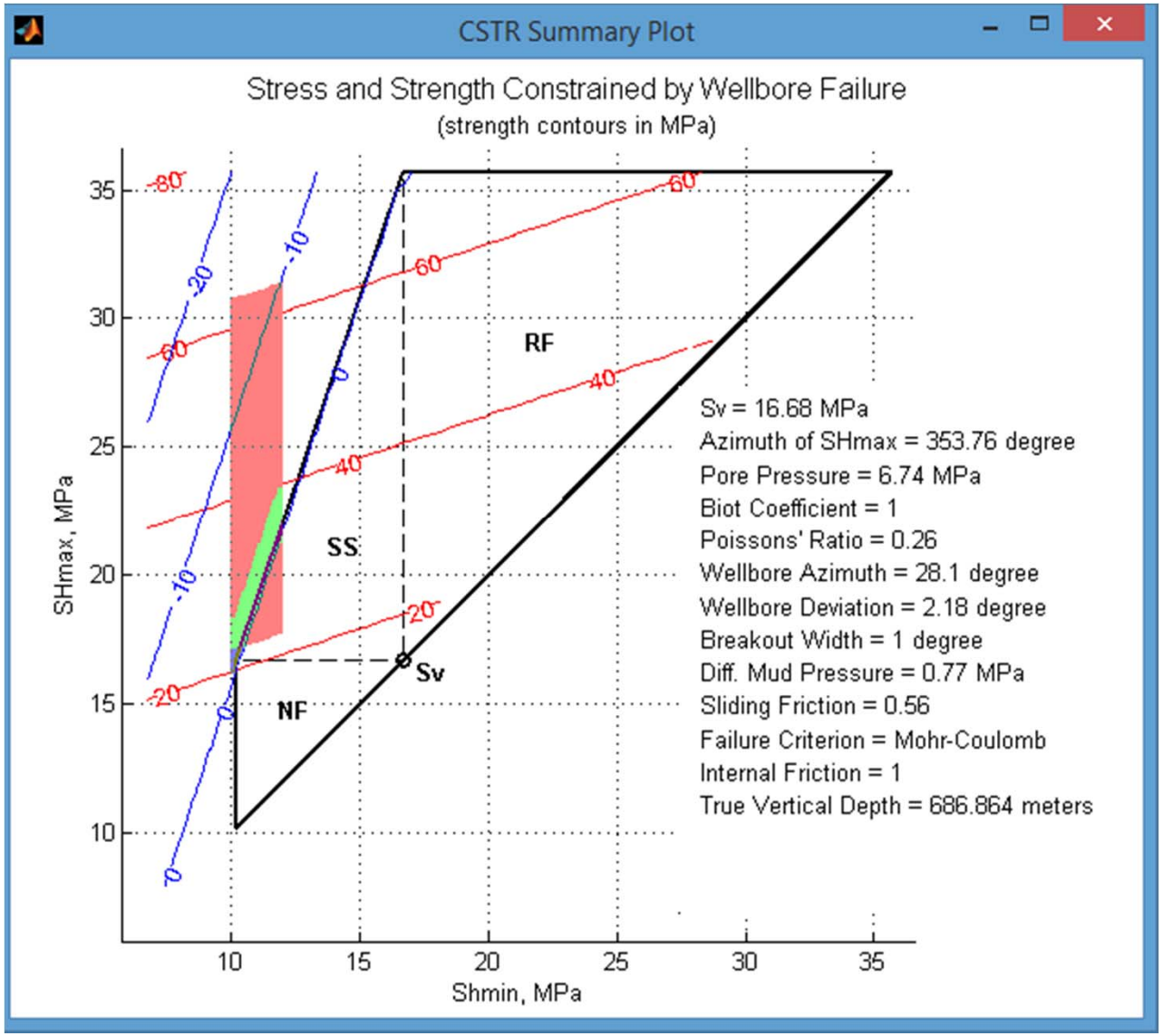

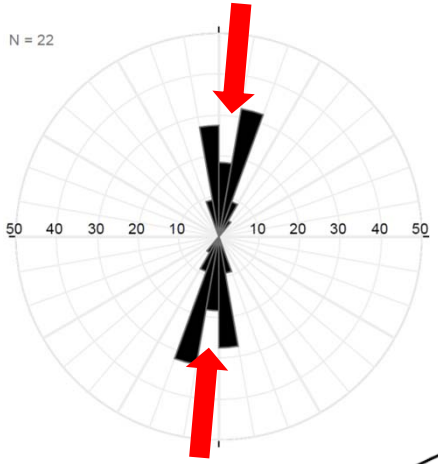

Open-Filling Fracture

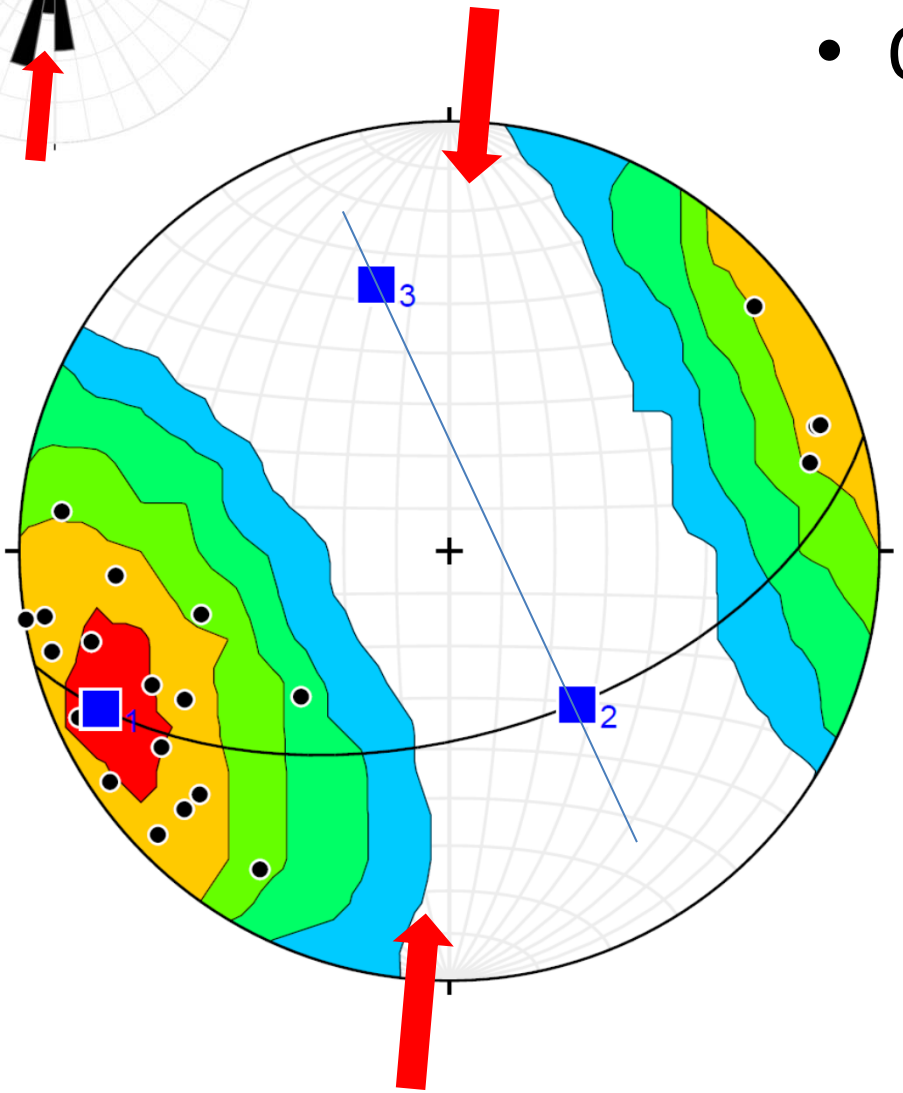

- Open-Filling Fracture
  \24.2W/78.2NE

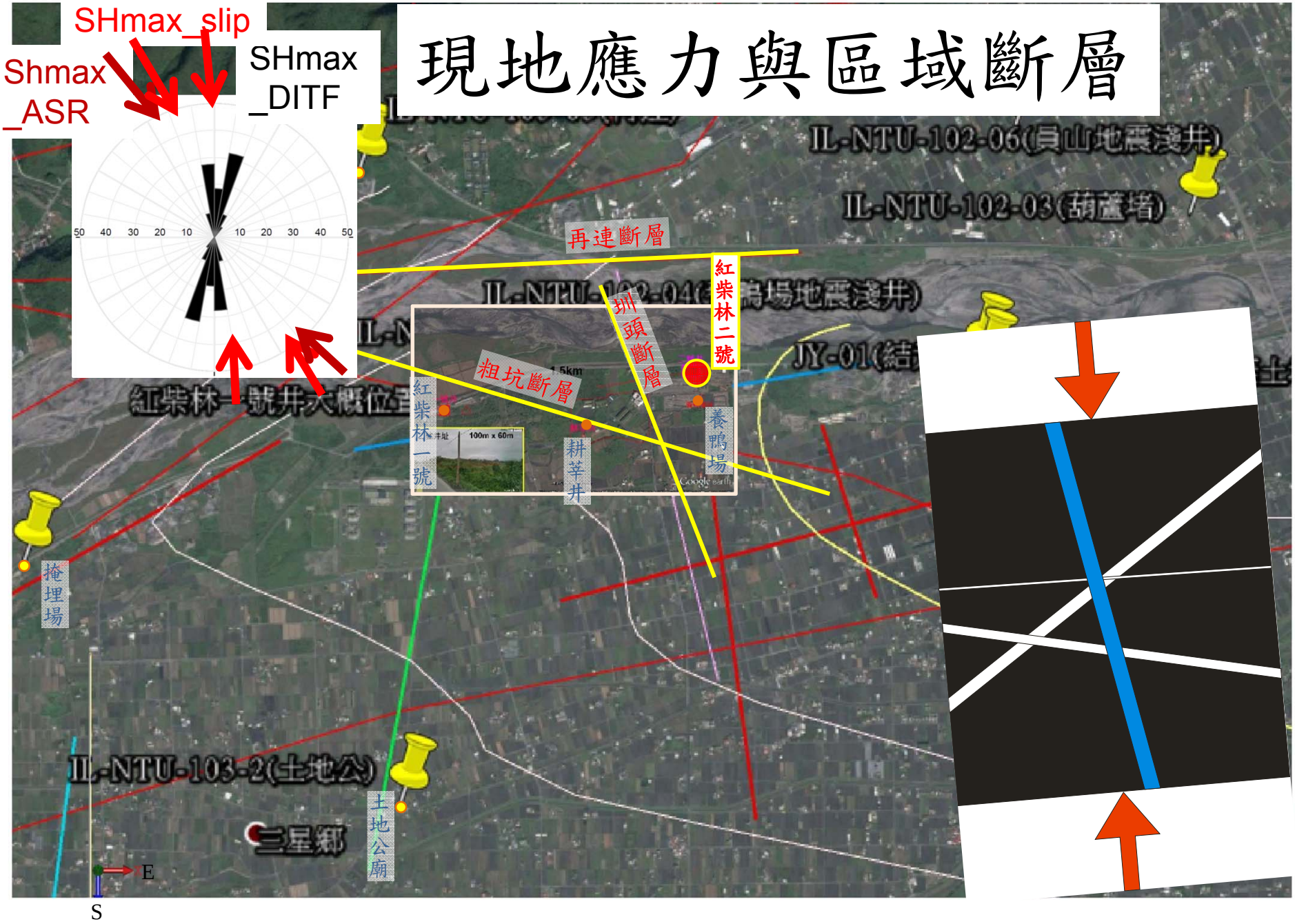
SHmax_slip
Shmax
_ASR
SHmax
_DITF
現地應力與區域斷層
IL-NTU-102-06(員山地震淺井)
IL-NTU-102-03(葫蘆堵)
再連斷層
紅柴林二號
圳頭斷層
粗坑斷層
紅柴林一號
耕莘井
養鴨場
掩埋場
IL-NTU-103-2(土地公)
土地公廟
三星鄉
E
S

Future Works

- Critical pressure perturbation
- Fault reactivation analysis
- Stress magnitude from focal mechanism

Critical Pressure Perturbation

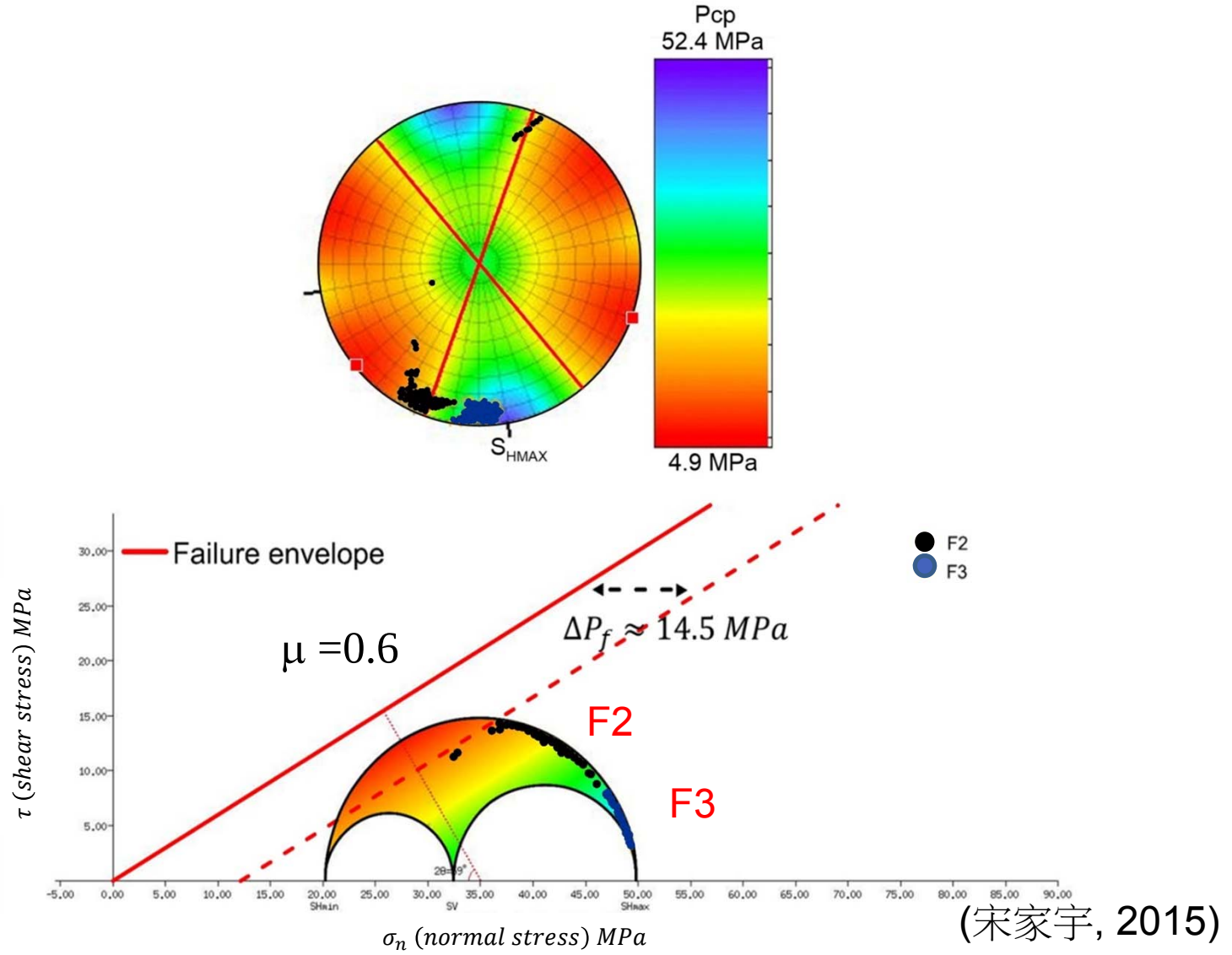

(宋家宇, 2015)

Fault Reactivation Analysis
Seismic Hazard

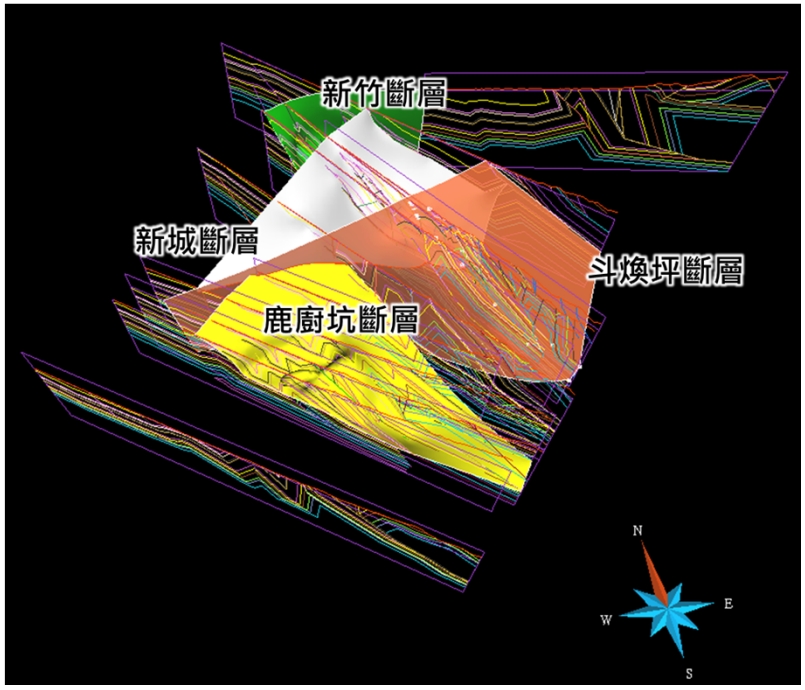

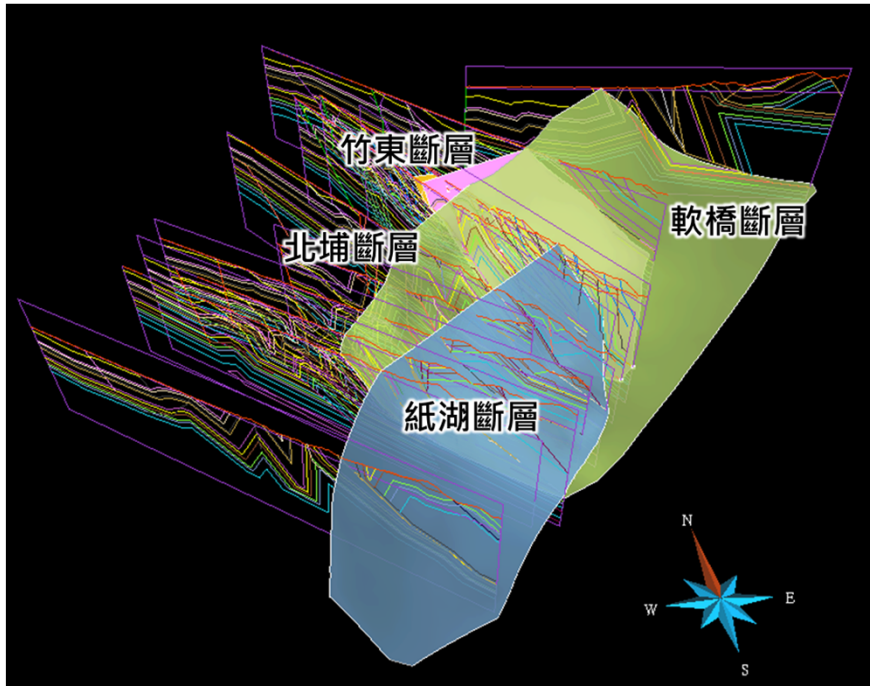

(國家災害防救科技中心, 2015)

Stress Magnitude from Focal Mechanism

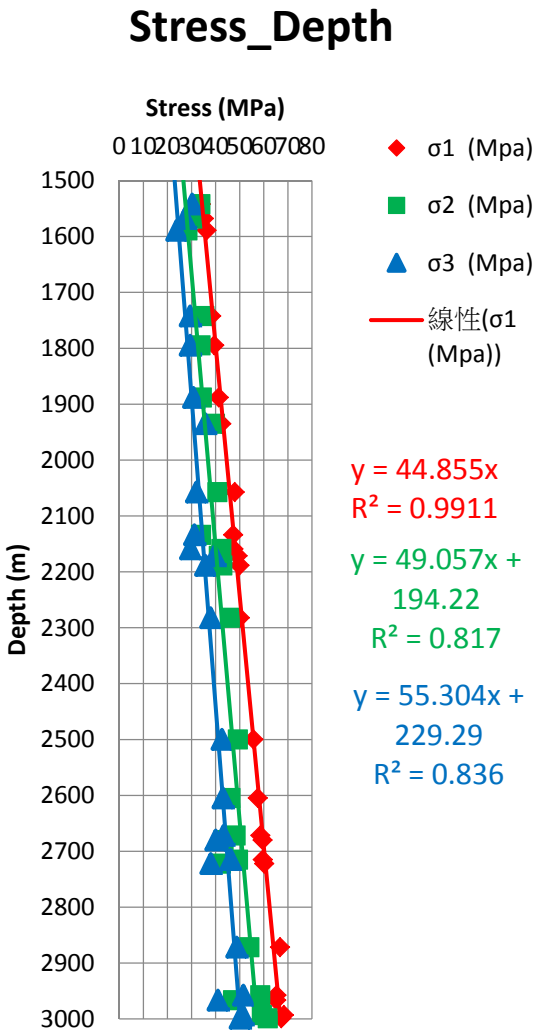

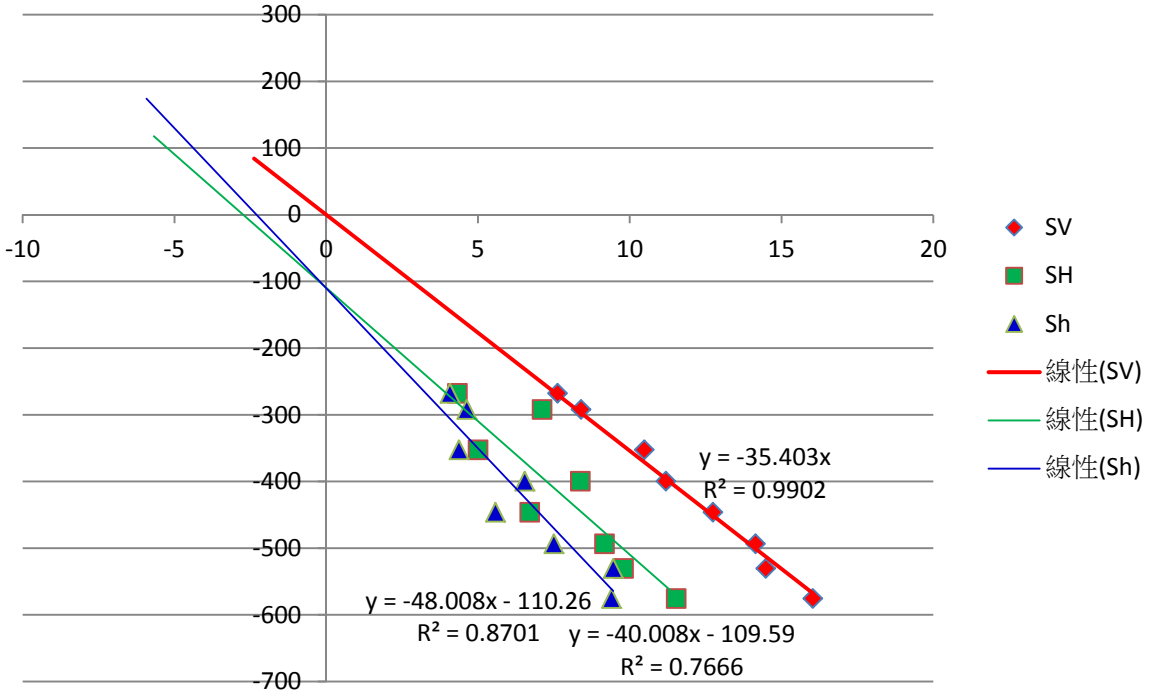

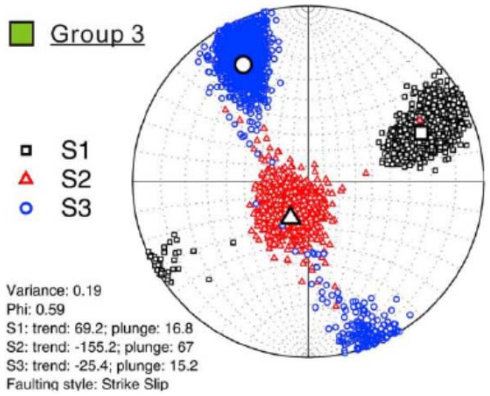

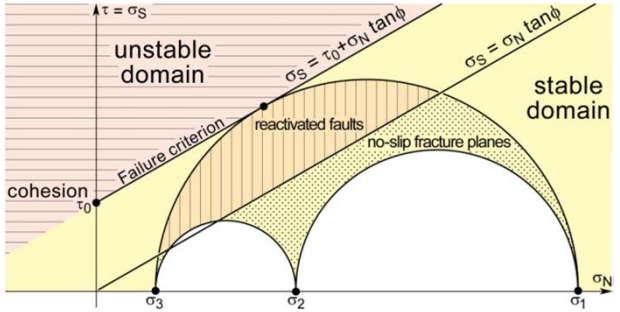

Domain of reactivated, inherited fractures in a Mohr diagram with the three principal stresses

Take-Home Messages

- Integrated stress assessments from various methods, it will be able to determine the stress state in multiple spatial-scales and stress gradient.
- Relationship between in-situ stress and fracture should be able to apply for various topics of solid earth sciences.

Thank you for your attention!!